A Novel Antibacterial Surface Coating of Polydimethylsiloxane Using Quaternary Ammonium Compound functionalized Poly(oligo(ethylene glycol) methyl ether methacrylate) Microgels

By

Luc Gauthier

A Thesis

Submitted to the School of Interdisciplinary Sciences

In Partial Fulfillment of the Requirements

For the Degree

Honours Bachelor of

Science

McMaster University

HONOURS BACHELOR OF SCIENCE (2024) McMaster University

School of Interdisciplinary Sciences Hamilton, Ontario

McMaster University, Hamilton, ON

TITLE: A Novel Antibacterial Surface Coating of Polydimethylsiloxane Using Quaternary Ammonium Compound functionalized Poly(oligo(ethylene glycol) methyl ether methacrylate) Microgels

AUTHOR: Luc Gauthier

SUPERVISORS: Dr. Todd Hoare, Mya Sharma

Number of Pages: x, 71

Abstract

Biofilms are a growing concern for medical implants and food processing because they can cause infections and resist antibiotics. One surface on which biofilms can form is polydimethylsiloxane (PDMS), a type of silicone rubber, which is often used for medical and food processing applications. The aim of this project is to prevent biofilm growth on PDMS by creating an antimicrobial surface coating based on microgels prepared using the anti-fouling polymer poly(oligoethylene glycol methacrylate) (POEGMA). These polymers were further functionalized with quaternary ammonium compounds (QACs) to incorporate antibacterial properties to reduce biofilm formation. The QAC-functionalized microgels were assembled in water and phosphate buffered saline (PBS) and were found to be stable over 20 days, with an average diameter of 240 nm. They also demonstrated excellent antimicrobial properties against both *Staphylococcus aureus* and *Pseudomonas aeruginosa* (Gram positive and negative respectively). The microgels showed a 9.56 log reduction (99.99999997% kill) against *S. aureus* and an 8.5 log reduction (99.999999% kill) against *P. aeruginosa*. To attach the microgels to PDMS, the PDMS was plasma treated to enable electrostatic binding between the originally hydrophobic PDMS and the cationic QAC-functionalized microgels. The effective immobilization of the microgels was confirmed using bromophenol blue (which turns blue in the presence of QACs) and atomic force microscopy (AFM). Finally, the microgel-coated PDMS demonstrated a 95% reduction of *S. aureus* which indicates this coating can sanitize PDMS. Future studies should be completed for microgel-PDMS bond strength and antimicrobial properties of PDMS-bound microgels. Ultimately, the QAC-functionalized POEGMA microgels were effective as an antibacterial coating on PDMS and could have applications such as a surface cleaner or a sterilizing agent to reduce the transmission of bacteria and prevent infections.

Acknowledgements

I would like to thank my supervisor Dr. Todd Hoare for his mentorship and guidance throughout my thesis project. Working in the Hoare lab has been an amazing experience, and I am glad to have had this wonderful opportunity. I would like to especially thank Mya Sharma, my direct supervisor, who helped me with her vast knowledge, guidance, and mentorship throughout the project. She has been instrumental throughout the project I am extremely grateful. I would like to thank all the members of the Hoare lab who trained me and helped with experiments.

I would also like to thank the School of Interdisciplinary Science for guiding me throughout these past four years. The Integrated Science program is truly one-of-a-kind, and I am glad to have been part of this amazing community.

I would like to thank my family and friends for all their support throughout the project, and throughout my undergraduate career. I would not be where I am today without you.

Table of Contents

List of Illustrations and Diagrams

List of Abbreviations and Symbols

DNA	Deoxyribonucleic acid
EPS	Extracellular polymeric substances
PDMS	Polydimethylsiloxane
PvdQ	An acylase form *Pseudomonas aeruginosa* PAO1
S-PDMS	Swollen-PDMS
SOCAL	Slippery omniphobic covalently attached liquid-like
PIMs	Polyimidazoliums, a type of antibiotic
PBS	Phosphate buffered saline
PNIPAM	Poly(N-isopropylacryliamide)
LCST	Lower critical solution temperature
POEGMA	Poly(oligo(ethylene glycol) methyl ether methacrylate)
OEGMA	(oligo(ethylene glycol)
$M(EO)_2MA$	(di-(ethylene glycol) methyl ether methacrylate)
Mol%	Mole fraction
QAS	Quaternary ammonium salt
QAC	Quaternary ammonium compound
AA	Acrylic acid
AIBMe	2,2-azobisisobutryic acid dimethyl ester
TGA	Thioglycolic acid
DMF	N, N-dimethylformamide
DMF:TFA	N, N-dimethylformamide: Trifluoroacetic acid
ADH	Adipic dihydrazide

EDC	1-(3-dimethylaminopropyl)-carbodiimide hydrochloride
MiQ	Milli-Q water
UV-Vis	Ultraviolet-visible spectroscopy
POHQ	QAC-Hydrazide-functionalized POEGMA ($PO_{30}H_{30}Q_{30}$)
POA	Aldehyde-functionalized POEGMA ($PO_{30}A_{30}$)
DLS	Dynamic Light Scattering
PDI	Polydispersity index
LB agar/broth	Luria-Bertani agar/broth
CFU	Colony-forming units
MTS	3-(4,5-dimethylthiazol-2-yl)-5-(3-carboxymethoxyphenyl)-2-(4-sulfophenyl)-2H-tetrazolium
FBS	Fetal bovine serum
PES	Phenazine ethyl sulfate
BPB	Bromophenol blue
AFM	Atomic force microscopy
SEM	Scanning electron microscopy
ASTM	American Society for Testing and Materials
OD600	Optical density 600 (nm)

1. Introduction

1.1 Biofilms

Biofilms are accumulations of microbes that adhere and proliferate on surfaces (Donlan, 2002). The microbes that comprise biofilms secrete extracellular polymeric substances (EPS) which allows them to gain protection against the environment and antibiotics (Abebe, 2020). EPS are high molecular weight organic polymers, usually comprised of polysaccharides, proteins, lipids, and extracellular DNA (Di Martino, 2018). Bacteria in biofilms are usually encased in EPS which helps prevent other organisms, environmental substances, or antibiotics from attacking their cellular targets (Muhammad et al., 2020). Due to their EPS secretion biofilms can exhibit up to an a thousand fold increase in antibiotic resistance compared to similar bacteria in a non-colony state (Lewis, 2008). This makes them an important consideration in biomedical and food processing applications (Liu et al., 2023). While there are many species that can form biofilms, the main species are *Pseudomonas aeruginosa*, *Staphylococcus aureus*, and *Staphylococcus epidermis* (Muhammad et al., 2020). Biofilms can range in composition of species but will usually see an abundance of at least 25% of the previously mentioned species for mixed biofilms (Alves et al., 2018). Mixed biofilms are more common than those made with individual species and are also far more virulent (Kvich et al., 2020). Biofilms tend to initially adhere and form in very humid areas (100% relative humidity) with temperatures between 30 and 40 °C (Else et al., 2003). They also prefer a pH levels near 7 during deposition but can gain protection against acidic or basic conditions through EPS secretion and encasing (Else et al., 2003). A biofilm also allows for horizontal gene transfer between resident bacteria, allowing them to adapt efficiently to their environment, overall ensuring their survival (Jefferson, 2004).

Biofilm formation and maturation usually occur in four stages: initial (reversible) attachment, adherence (irreversible), proliferation and maturation, and dispersal (Muhammad et al., 2020). A schematic of biofilm formation is observed in Figure 1.

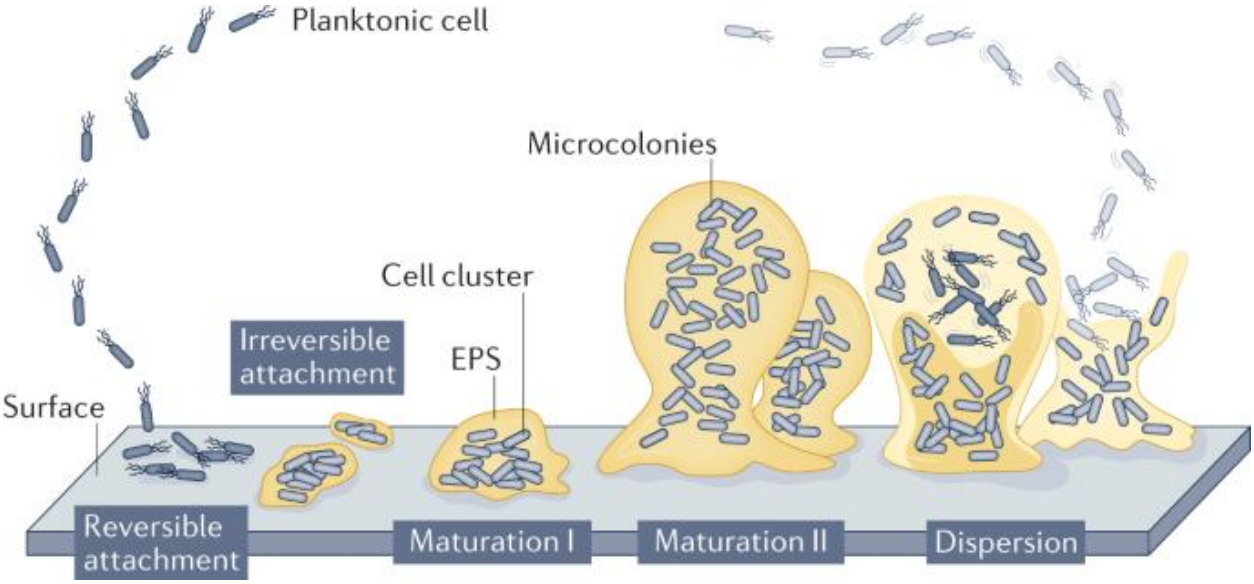

Figure 1. Schematic of biofilm formation. This schematic highlights the four major stages of biofilm development: reversible attachment, irreversible attachment, maturation I and II, and dispersion (Stoodley et al., 2002).

In the initial attachment stage bacteria will bind to surfaces using non-specific physical forces such as Van der Waals forces, electrostatic interactions, and hydrophobic interactions (Jesmer et al., 2023). Bacteria are more likely to bind to rough, porous surfaces (Jesmer et al., 2023). In the adherence stage bacteria will employ surface adhesins such as pili, fimbriae, and capsules to irreversibly bind to the surface (Gordon & Wang, 2019). Once bound, the bacteria will take nutrients from the environment which allows them to grow and proliferate. This leads to the secretion of EPS as a result of quorum sensing (Muhammad et al., 2020). Quorum sensing is a type of cellular communication between bacteria using signal molecules that increase in concentration with increased cell density and changes in the physiological environment (Elias & Banin, 2012). This communication usually leads to changes in gene transcription which cause the

release of EPS into their environment (Di Martino, 2018). This is the stage at which the bacteria become protected from the environment and antibiotics. Finally, as the biofilm gets larger, it will mature and individuals or small clumps from the colony can disperse to infect other areas (Muhammad et al., 2020).

Biofilms can be found in non-host environments such as industrial or potable waterpipes, natural water sources (streams, ponds, and lakes), and food processing surfaces (wood, plastic, stainless steel, and glass) (Carrascosa et al., 2021; Donlan, 2002). Biofilms can exist in food processing plants, where they become a source of cross-contamination and cause disease (Abebe, 2020). They can also arise in host environments such as implanted medical materials like catheters, pacemakers, and contact lenses (Wu et al., 2015). In fact, biofilms are thought to be responsible for 80% of all chronic infections in humans (Assefa & Amare, 2022). They are thought to arise from natural infection due to the materials' exposure to the environment, and rarely, infections from surgery (Khatoon et al., 2018). Biofilms can also form in microfluidic systems which have important considerations in drug delivery, cell culturing, and nanoparticle fabrication (Niculescu et al., 2021). Biofilms are an important consideration in biomedical, food processing, and microfluidic applications due to their ability to potentially harm individuals (Liu et al., 2023). Thus, reducing biofilms is a major focus of research worldwide (Subhadra et al., 2018).

1.2 Biofilms and Polydimethylsiloxane (PDMS)

PDMS is a silicone elastomer widely used in microfluidics, microelectromechanical systems, biomedical devices, medical implants, and optical systems (Kumar & Kumar Sahani, 2021; L. Liu & Sheardown, 2005; van Poll et al., 2007). This is due to PDMS's excellent tissue compatibility, optical transparency, resistance to biodegradation, and simple and low-cost

fabrication (Miranda et al., 2021). Due to its natural smooth hydrophobic surface, PDMS also has inherent antifouling properties (Armugam et al., 2021). Antifouling is the prevention of adhesion of unwanted organisms to a surface (Romeu & Mergulhão, 2023). Despite its many characteristics and uses, PDMS has several disadvantages. In particular, despite its antifouling properties, bacteria are able to adhere and grow on PDMS surfaces (Vogel et al., 2020). Several bacterial species have been observed to bind PDMS, notably, *Escherichia coli*, *P. aeruginosa* (both Gram-negative), and *S. aureus* (Gram-positive) (Cont et al., 2023; Tu et al., 2019). *S. aureus* has been observed to bind to abiotic hydrophobic surfaces (such as PDMS) with many weakly-binding, low-affinity ligands (Maikranz et al., 2020). Conversely, this species tends to bind to hydrophilic surfaces using a small number of high-affinity ligands (Maikranz et al., 2020). *P. aeruginosa* and *E. coli* have been observed to preferentially bind to abiotic hydrophobic and hydrophilic surfaces respectively, with high affinity (Hamadi et al., 2008; Zabielska et al., 2017). *P. aeruginosa* and *E. coli* can also bind to hydrophilic and hydrophobic surfaces respectively, albeit, with lower affinity (Hamadi et al., 2008; Zabielska et al., 2017). These differing binding types allow bacteria to adhere and thrive in a variety of different environments, making these variations in binding an important consideration in biofilm reduction.

1.3 Biofilm Regulation Methods for PDMS

Limiting the formation of biofilms or bacterial colonies on PDMS surfaces has been an important consideration in research for decades (Fux et al., 2005; Miranda et al., 2021). Antibiofilm techniques usually employ one or more of the following mechanisms: replacing the material that host biofilms, prevention of adhesion (also known as antifouling), direct killing with antibiotics or phages, and surface modification of the substrate material (De Luca et al., 2022;

Mishra et al., 2020; Wu et al., 2015; Zhao et al., 2020; Zhu et al., 2022). These strategies are sometimes used in combination to ensure biofilms are eradicated and prevent them from returning. Most strategies focus on preventing adhesion, usually through modification of the substratum to induce contact killing.

A study by Vogel et al. (2020) demonstrated how the surface modification of PDMS with PvdQ led to reduced *P. aeruginosa* growth. PvdQ is an acylase expressed by *P. aeruginosa*, involved in quorum sensing in biofilms containing these bacteria. Quorum sensing molecules change the gene expression of bacteria based on population density and often cause increased virulence (Vogel et al., 2020). PvdQ is known as a quorum quencher for *P. aeruginosa* leading to the downregulation of virulence factors, reducing its severity of infection (Utari et al., 2018). Vogel et al. (2020) plasma treated the PDMS surface to increase hydrophilicity by creating hydroxyl groups, and then coated it with PvdQ. They found a 50% reduction in *P. aeruginosa* growth compared to untreated PDMS. Thus, the surface treatment of PDMS caused reduced growth of *P. aeruginosa* on their samples, but it was not effective enough to be an applicable method for surface sanitization, which is normally a 95% reduction in bacteria (Altapure, 2024).

A study by Zhu et al. (2022) investigated the treatment of PDMS to make it superhydrophobic in order to prevent bacterial growth. Their study consisted of infusing silicone oil (an organic hydrophobic lubricant) into the PDMS crosslinks to make a swollen PDMS network. A schematic of this can be observed in Figure 2. Zhu et al. (2022) also tested a slippery omniphobic covalently attached liquid-like (SOCAL) surface on PDMS. An omniphobic substance is one that repels all liquids, regardless of their surface tension (Zhu et al., 2022). They made their SOCAL treatment through an acid-catalyzed graft polycondensation of PDMS. They assessed *P. aeruginosa* growth on SOCAL and S-PDMS and found that it led to 95.0 ± 4.3 % and

88.7 ± 11.0% reductions in bacterial growth, respectively. This shows that surface modification of PDMS by making it more hydrophobic effectively reduced bacterial adhesion. However, while extremely reduced compared to non-infused PDMS controls, the authors still saw biofilm formation over a 7-day period (Zhu et al., 2022).

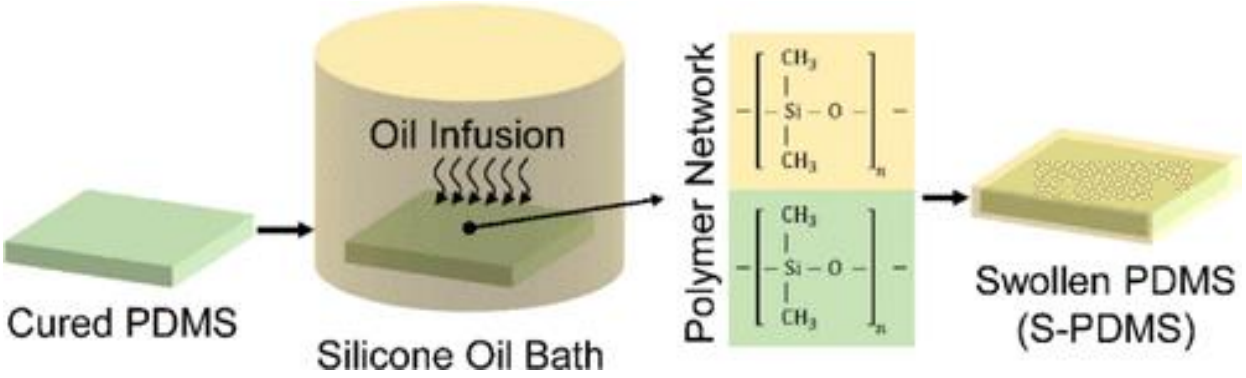

Figure 2. Schematic diagram for fabricating S-PDMS prepared by infusing PDMS with silicone oil. This diagram highlights the different layers of PDMS leading to formation of S-PDMS, a superhydrophobic surface. First, the PDMS is created, then it is infused with silicone oil, creating a network of oil within the polymer structure. (Zhu et al., 2022).

Armugam et al. (2021) decided to take another direction by integrating a broad-spectrum antibiotic into the PDMS for controlled release. The authors used polyimidazoliums (PIMs), a type of biocompatible antibiotic effective against *S. aureus* and *P. aeruginosa* (Zhong et al., 2020). First, they synthesized a PIM-vinyl polymer which was mixed with the PDMS base before the addition of the curing agent. This addition yielded a composite PIM-PDMS material. The resulting material was shown to gradually release the antibiotic for effective killing of *E. coli* and *P. aeruginosa*. In fact, the authors found an average of a 6 log reduction (99.9999% kill) during antibacterial tests and that the substance had substantial killing for up to 30 days (Zhong et al., 2020). These results show a promising application toward biofilms in medical implants but can be a concern when it comes to antibiotic resistance. Since bacteria can mutate and quickly gain

resistance against antibiotics (Lewis, 2008), a combined use of antimicrobials and antifouling agents would be an ideal choice.

1.4 Microgels for Combined Biofilm Regulation

Using the combined effects of antimicrobials and natural antifouling properties for PDMS is a better approach to reducing or eliminating biofilm formation. There are many methods to achieve this goal such as grafting polymer brushes to PDMS (Sun et al., 2022; van Poll et al., 2007), coating the surface with antimicrobial surfactants (Stepulane et al., 2022), and notably, coating the surface with antimicrobial microgels (Keskin et al., 2020; Zhao et al., 2020).

Microgels are three dimensional hydrophilic networks of crosslinked polymers (Wechsler et al., 2019). Microgels do not dissolve in water or phosphate buffered saline (PBS) due to their crosslinking, meaning the solvent can enter the crosslinks and swell the network (Peppas et al., 2006). Microgels are widely accepted as hydrogels with a size of 100 nm to 1 μm (de Lima et al., 2020). Several polymers have been used to create microgels, including thermoresponsive polymers such as Poly(N-isopropylacryliamide) (PNIPAM) and Poly(oligo(ethylene glycol) methyl ether methacrylate) (POEGMA). The former can be functionalized with various biocidal agents, such as quaternary ammonium compounds (QACs), to enhance its antibacterial properties.

1.5 Quaternary Ammonium Compounds (QACs)

QACs are highly effective biocidal chemicals widely used in cleaners and disinfectants (Arnold et al., 2023). Their structure consists of a quaternary ammonium group with alkyl or aromatic groups of chain lengths between 8 and 18 carbon atoms (Alihosseini & Sun, 2011). They work by infiltrating the cellular membrane with the help of their hydrophobic side chains and disrupt it using their positively charged ammonium group (Arnold et al., 2023). This disruption

can eventually cause cell lysis and death (Schrank et al., 2020). Their mechanism of action can be observed in Figure 3.

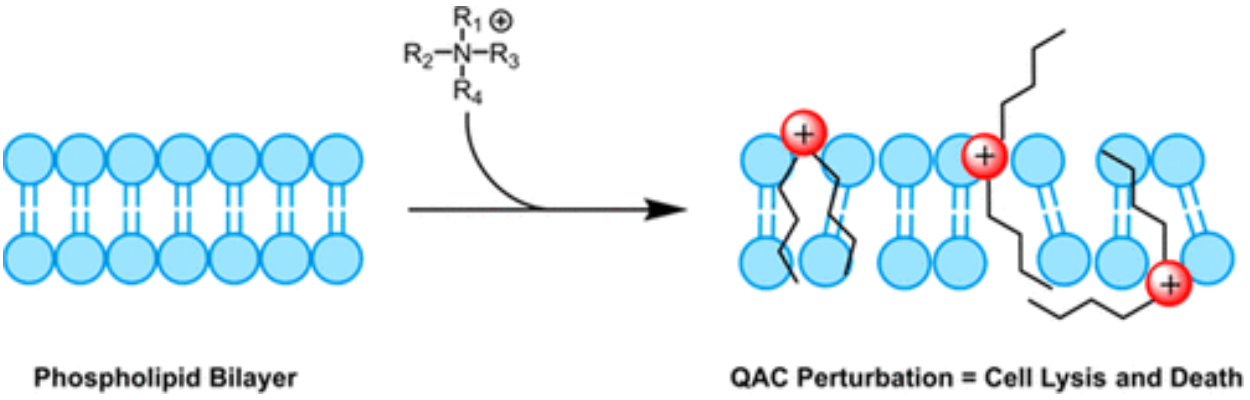

Figure 3. The mechanism of action of quaternary ammonium compounds. QACs infiltrate the plasma membrane and cause perturbation, leading to cell lysis and death (Schrank et al., 2020).

While there are several types of QACs they all have similar structures. For example, quaternary ammonium salts (QASs) usually have an anion paired with the ammonium cation in solution to keep them stable (Mohapatra et al., 2023). For simplicity, these compounds will be referred to as QACs throughout this paper.

1.6 PNIPAM Microgels

PNIPAM is a soft, thermoresponsive polymer that is widely used in drug delivery, biosensors, and implanted materials (Guan & Zhang, 2011). These polymers can create hydrogels with highly tunable sizes. PNIPAM is also known to have inherent antifouling properties, which makes it an attractive substance for biological applications (Pan et al., 2022). PNIPAM is thermoresponsive because it has a lower critical solution temperature (LCST). The LCST is defined as the minimum temperature at which the immiscible phase transition of a polymer occurs

(Zhang et al., 2021). In other words, above this temperature, the polymer begins to aggregate together and becomes immiscible in the solvent. An LCST phase diagram is seen in Figure 4.

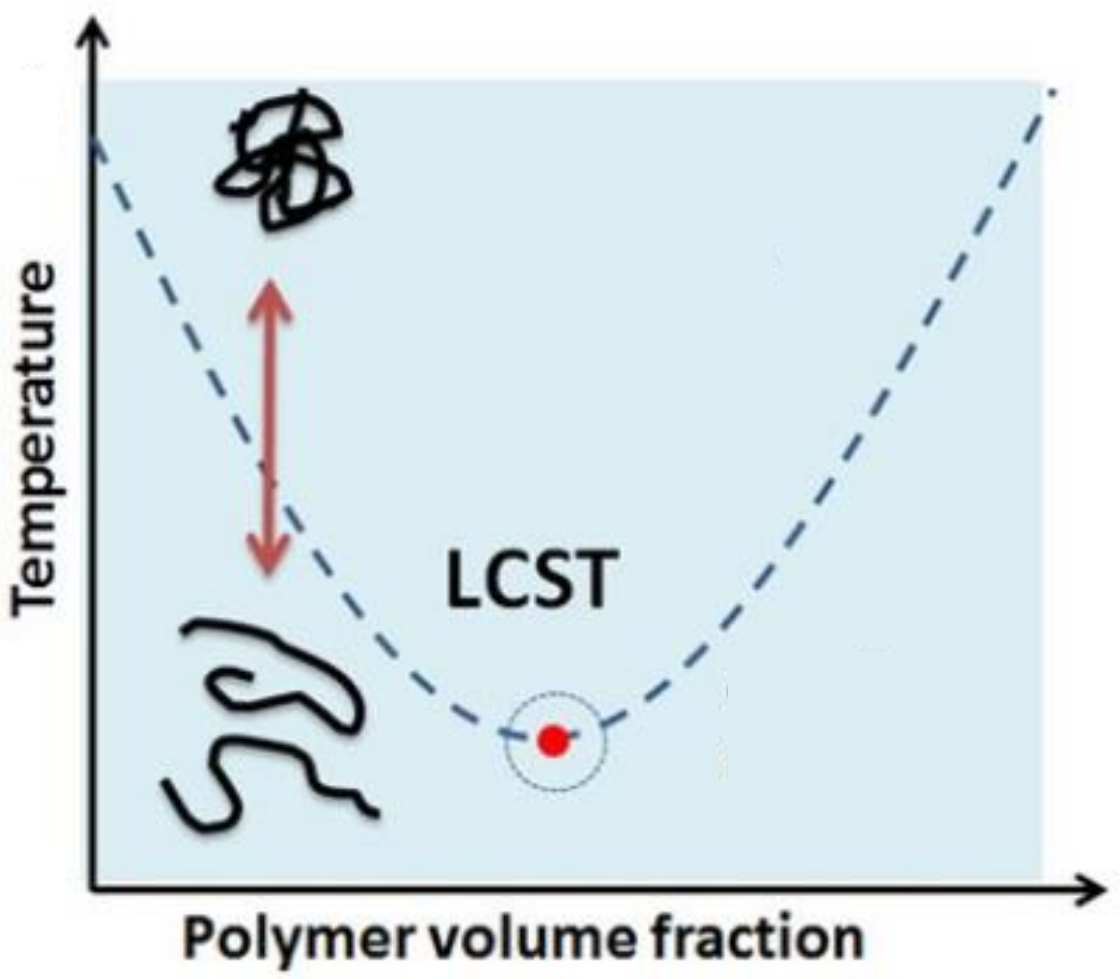

Figure 4. A phase diagram for a polymer solution exhibiting an LCST. The horizontal axis is the polymer concentration (increasing to the right), and the vertical axis is the temperature (increasing upwards). The dashed line represents the binodal, or the threshold at which the miscible to immiscible phase transition occurs. The LCST is represented as the red dot, or the lowest temperature at which this phase transition occurs. Adapted from Koçak et al. (2020).

Figure 4 highlights the binodal as a dashed line. This is the temperature threshold at which the miscible to immiscible phase transition occurs. The LCST is represented as the red dot, or the

lowest temperature at which this transition occurs. PNIPAM has an LSCT of about 32 °C, which makes it an extremely biologically relevant polymer (Jain et al., 2015).

PNIPAM microgels are usually created by precipitation polymerization (Hu et al., 2011). This is a process by which PNIPAM polymers are nucleated homogenously, with the polymerization occurring at temperatures of 60°C to 70 °C, above its LCST. This is to encourage aggregation and precipitation of the polymers into a nanoparticle structure (Hu et al., 2011).

Zhao et al (2020) synthesized PNIPAM microgels functionalized with QACs, an excellent biocidal agent (Jia et al., 2001). As previously mentioned, QACs are able to electrostatically adhere to bacteria, and their hydrophobic chains can penetrate the cell membrane and cause death (Ding et al., 2015). Thus, their functionalization to PNIPAM microgels made them inherently antimicrobial. Zhao et al. (2020) investigated the formation of a PNIPAM-QAC film formation on PDMS to observe its application for antimicrobial implanted materials. They observed a bactericidal efficacy of 99.9 ± 0.2% against *E. coli*. Fluorescent micrographs and atomic force microscopy (AFM) showed even distribution of bacterial killing and microgel placement. They also demonstrated that their PNIPAM-QAC microgels were highly biocompatible, making them a promising coating for implanted materials (Zhao et al., 2020). However, PNIPAM hydrogels also have disadvantages such as poor mechanical strength, relatively non-tunable LCST (for implanted material applications), and lower microgel stability in the body compared to POEGMA (Ansari et al., 2022; Xu et al., 2020). Thus, the use of POEGMA has been actively research as an advantageous alternative to PNIPAM.

1.7 POEGMA Microgels

POEGMA, is a highly tunable, tissue compatible, and thermoresponsive polymer (Simpson et al., 2018). POEGMA polymers are easy to fabricate and highly tissue compatible (non-toxic and non-immunogenic), more so than its PNIPAM counterpart (Vihola et al., 2005). POEGMA polymers also show good antifouling properties, reducing bacterial cell adhesion by an average of 75% (Jesmer et al., 2023). These polymers have an LCST that ranges between 30 °C and 90 °C, depending on the co-polymers used in its structure (Zuppardi et al., 2020). POEGMA polymers are usually made from two major co-polymers, OEGMA (oligo(ethylene glycol) methyl ether methacrylate) and $M(EO)_2MA$ (di-(ethylene glycol) methyl ether methacrylate). Higher mol% of OEGMA in the polymer sequence increases the LCST of the overall polymer (Zuppardi et al., 2020). This makes POEGMA highly tunable and biocompatible, elucidating why it is often used in implanted biomaterials, tissue engineering, and drug delivery (Smeets et al., 2014). Moreover, POEGMA can be functionalized with hydrazide and aldehyde groups which create hydrazone bonds and cause crosslinking of the polymers (Simpson et al., 2018). This is key to the synthesis of hydrogels and microgels.

POEGMA microgels can be created in different ways but the most common is through self-assembly using its thermoresponsive properties (Smeets et al., 2014). Depending on which copolymer is used in abundance (OEGMA or $M(EO)_2MA$), the LCST of POEGMA can be easily modified for specific applications. Due to their inherent ability to aggregate and precipitate, the POEGMA polymers can simply be heated above their LCST to create homogenous microgels.

Several studies have investigated applications of POEGMA polymer brushes as antifouling coatings for PDMS (Jesmer et al., 2023), and antibacterial coatings along with other nanoparticles (Nastyshyn et al., 2020). These studies showed 75-90% reduction of bacterial adhesion and

complete sanitization (6 log reduction), respectively (Altapure, 2024; Jesmer et al., 2023; Nastyshyn et al., 2020). However, the use of POEGMA microgels as antibacterial coating of PDMS is rarely seen in the literature. Due to their inherent tissue compatibility, easy synthesis, and high adjustability, POEGMA microgels with QACs are interesting candidates for biofilm prevention on PDMS. This method could prove highly effective against biofilms that form on PDMS, reducing the risk of infections in the various applications where PDMS is used.

1.8 Novel QAC-functionalized POEGMA Microgels for Biofilm Reduction on PDMS

Here we address the issue of biofilm formation on PDMS through the use of QAC-functionalized POEGMA microgels. We will assess if they can bind and coat the surface of PDMS and assess their antimicrobial properties. This will be done through the synthesis of QAC-functionalized POEGMA polymers and their eventual self-assembly into microgels, using methods developed by the Hoare lab. Using these methods, the goal is to synthesize a tissue compatible antimicrobial microgel coating of PDMS. The PDMS will be plasma treated to create hydroxyl groups on its surface to enable electrostatic binding with the microgels. Finally, we assess the antimicrobial properties of the microgel coating and highlight its potential applications. This novel coating could reduce the formation of biofilms on PDMS and ensure a sterile surface is obtained.

2 Materials and Methods

2.1 Materials

Oligo(ethylene glycol) methacrylate (OEGMA*475*, EO repeats = 8−9) was purchased from Millipore Sigma and purified by running the monomer through a column of aluminum oxide

(MilliporeSigma) to remove the inhibitors. Acrylic acid (AA, MilliporeSigma), dimethyl 2,2'-azobis(2-methylpropionate) (AIBMe, Pure Chemistry Scientific Inc.), thioglycolic acid (TGA, MilliporeSigma), dimethylformamide (DMF, Caledon Laboratories Ltd.), adipic acid dihydrazide (ADH, AK Scientific), N′-ethyl-N-(3-(dimethylamino)propyl)-carbodiimide (EDC, MilliporeSigma), N-(2-(methacryloyloxy)ethyl)-N,N-dimethyldodecan-1-aminium bromide (MilliporeSigma), 2-dimethylaminoethyl methacrylate (MilliporeSigma), 1-bromododecane (MilliporeSigma), acetonitrile (MilliporeSigma), diethyl ether (MilliporeSigma), ethyl acetate (MilliporeSigma), Luria-Bertani broth (LB, PhytoTech Labs), agar (BioShop Canada Inc.), Letheen Broth (MilliporeSigma), polysorbate 80 (MilliporeSigma), L-α-Lecithin (Millipore Sigma), fetal bovine serum (FBS, MilliporeSigma), Dulbecco's Modified Eagle Medium (MilliporeSigma), and 3-(4,5-dimethylthiazol-2-yl)-5-(3-carboxymethoxyphenyl)-2-(4-sulfophenyl)-2H-tetrazolium (MTS, MilliporeSigma). were all used as received. *Pseudomonas aeruginosa* (ATCC 15442), and *Staphylococcus aureus* (ATCC 6538) were used in biological experiments. Milli-Q grade distilled deionized water (DIW, 18.2 MΩ cm resistivity) was used in all syntheses and double distilled water was used in all biological experiments. A Sylgard 184 commercial kit (Sigma-Aldrich) was used for PDMS fabrication.

2.2 Synthesis of QAC Monomer

The QAC monomer used in study is N-(2-(methacryloyloxy)ethyl)-N-N-dimethyldodecan-1-aminium bromide. It was synthesized by first adding 2-dimethylaminoethyl methacrylate (5.36 mL, 31.8 mmol) to 1-bromododecane (6.87 mL, 28.6 mmol) into 20 mL of acetonitrile. The reaction was stirred at 40 ℃ for 24 hours in a nitrogen environment, removing any oxygen present.

Once completed, the reaction was rotary evaporated and filtered using 60 mL diethyl ether. Finally, the QACs were recrystallized and filtered using ethyl acetate.

2.3 Synthesis of Hydrazide-QAC-functionalized and Aldehyde-functionalized POEGMA

The hydrazide-QAC-functionalized polymer was synthesized to have 30 mol% hydrazide functional groups and 30 mol% QAC groups. The polymer was also synthesized to have 30 mol% of $OEGMA_{475}$ (oligo(ethylene glycol) methyl ether methacrylate), average molecular weight of 475 g/mol) and 70% $M(EO)_2MA$ (di-(ethylene glycol) methyl ether methacrylate), yielding an overall polymer denoted as $PO_{30}H_{30}Q_{30}$. The polymers were synthesized with the mass of each reagent outlined in Table 1. Briefly, $OEGMA_{475}$, $M(EO)_2MA$, hydrazide monomer, QAC monomer, AIBMe, and TGA were added to a round bottom flask with 20 mL DMF. Then it was nitrogen purged for 30 minutes, submerged into an oil bath at 75℃, and let to stir at 400 rpm overnight. The next day, the solvent (DMF) was removed through rotary evaporation, and 5 mL of 50:50 DCM:TFA were added and stirred for 3 hours, before the solvent was blown off. Next, 100 mL of water was added and let stir overnight to dissolve, then the solution was dialyzed using 3.5 kDa molecular weight membranes for a minimum of 6 hours for 6 cycles. Once completed, the polymers were freeze-dried and dissolved in MiQ or PBS to have concentrations of 20 wt%.

The aldehyde-functionalized polymer was synthesized to have 30 mol% aldehyde-functional groups. It was also synthesized to have 30 mol% of $OEGMA_{475}$ and 70% $M(EO)_2MA$, yielding an overall polymer denoted as $PO_{30}A_{30}$. The polymers were synthesized with the mass of each reagent outlined in Table 1. Briefly, $OEGMA_{475}$, $M(EO)_2MA$, N-(2,2 DMEMAm) AA, AIBMe, and TGA were added to a round bottom flask with 20 mL DMF. Then it was nitrogen purged for 30 minutes, and submerged into an oil bath at 75℃, allowing it to stir at 400 rpm

overnight. The next day, the solvent (DMF) was removed through rotary evaporation, and 70 mL of water and 30 mL of 1M HCl was added and let stir overnight to dissolve. The solution was dialyzed using 3.5 kDa molecular weight membranes for a minimum of 6 hours for 6 cycles. Once completed, the polymers were freeze-dried and dissolved in MiQ or PBS to have concentrations of 20 wt%. The synthesis of these polymers can be observed in the synthesis schemes in Figure 5.

Table 1. Mass of reagents required for the synthesis of $PO_{30}H_{30}Q_{30}$ and $PO_{30}A_{30}$ polymers

Reagent	**Mass Required for $PO_{30}H_{30}Q_{30}$**	**Mass Required for $PO_{30}A_{30}$**
$OEGMA_{475}$	1.1 g (2.32 mmol)	1 g (2.11 mmol)
$M(EO)_2MA$	1.017 g (5.40 mmol)	0.9246 g (4.91 mmol)
Hydrazide monomer	1.1592 g (5.79 mmol)	0
AIBMe	56.294 mg	24.455 mg
QAC Monomer	2.3531 g (5.79 mmol)	0
N-(2,2 DMEMAm)	0	0.5209 m (3.01 mmol)
TGA	10.5 μL	2 μL
DMF	20 mL	20 mL

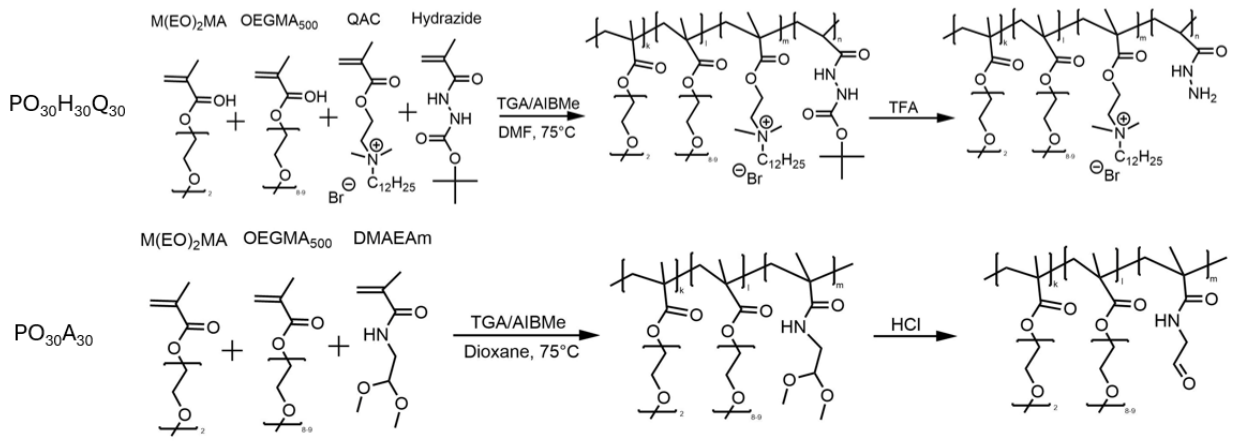

Figure 5. Synthesis schemes of $PO_{30}H_{30}Q_{30}$ and $PO_{30}A_{30}$ polymers. The top row shows the synthesis of $PO_{30}H_{30}Q_{30}$ with the addition of hydrazide and the QAC, and the bottom row shows the synthesis of $PO_{30}A_{30}$ with an aldehyde functionalization.

2.4 Lower Critical Solution Temperature (LCST) of POHQ and POA

The LCST of POHQ and POA were determined by Ultraviolet-Visible (UV-Vis) spectroscopy. Samples were prepared at 10 wt% $PO_{30}H_{30}Q_{30}$ or 10 wt% $PO_{30}A_{30}$ in MiQ and PBS. 3 mL of the samples was put into cuvettes, which were inserted into the UV-Vis spectrometer. The machine was set to take a measurement every 0.5 degrees, increasing the temperature at one degree per minute. The measurements began at 25℃ and ended and 99℃. The absorbance data was downloaded and converted to transmittance measurements in Excel.

2.5 Microgel Synthesis

Microgel synthesis was completed using the self-assembly method developed by the Hoare lab (Simpson et al., 2018). Microgel synthesis started with preparing 1 wt.% solutions of POHQ and POA in MiQ and PBS. A scintillation vial with 5 mL of 1 wt.% POHQ was placed into an oil bath at 87℃ (above the LCST of both polymers). It was heated for approximately 15 minutes with

magnetic stirring at 350 rpm until the internal temperature reached 85℃. Then, 1 mL of the POA crosslinker was added dropwise over about 30 seconds. The mixture was left to stir for 15 minutes and then taken out of the oil bath to let cool overnight at room temperature. The microgel solution was filtered using a 0.45-micron syringe filter to remove larger particle aggregations and other impurities. Microgel size, polydispersity, and stability was assessed using dynamic light scattering (DLS). Polydispersity was measured in PDI (polydispersity index). A PDI value of 0.2 was considered monodispersed.

2.6 Microgel Stability

Microgel stability was observed over a period of 20 days using DLS. Each sample was observed six times for size and polydispersity at 25℃ for 120 seconds for each run. The results were compiled as the average of the 6 attempts and inputted into Excel for analysis.

2.7 Microgel Antibacterial Properties

The antibacterial properties of the microgels were assessed using antibacterial tests with *S. aureus* and *P. aeruginosa*. First, starter plates were made by putting 10 µL of the stock *S. aureus* and *P. aeruginosa* on a petri dish with LB agar and streaking with a pipette tip. The starter plate was incubated at 37℃ and left to grow overnight. The next day, the bacterial streaks were suspended in the solution and were serially diluted to reach a final concentration of 10^6 CFU/mL (colony-forming units per mL). In a 96-well plate, the microgels were serially diluted in liquid LB media in columns 1-10. Once this was completed, 50 µL of 10^6 bacteria was added to each well. Column 11 was the negative control with 50 µL liquid LB media and 50 µL or bacteria. Column 12 was the positive control with just 100 µL of media. The plates were incubated at 37℃ overnight. The next day, the plates were put into a Tecan M200 plate reader to determine the concentration

of bacteria. The plate reader shines a 600 nm laser at the sample and measures absorbance, which is directly proportional to the concentration of bacteria in the sample.

2.8 Microgel cytotoxicity

Microgel cytotoxicity was determined using an MTS assay using murine 3T3 fibroblasts. First the cells were cultured and passaged. Then, 100 µL of Dulbecco's Modified Eagle Medium (with 10% FBS and 1% penicillin streptomycin) and 10^4 cells were added to each well of two 96-well plates (one for MiQ and one for PBS). The plates were then incubated at 37°C overnight. The microgels were filtered with a 0.45-micron filter in MiQ and PBS and 50 µL of microgels were added to their respective plates (MiQ or PBS). The wells were serially diluted by removing 50 µL from the previous well and adding it into the next well. This was completed from columns 1-10. Column 11 was the positive control with 10^4 3T3 fibroblasts and media, and column 12 was the negative control with just media. The plate was incubated again at 37°C overnight. The next day, 100 µL of media was removed from each well and 100 µL of fresh media was added. 20 µL of the MTS stain which contains phenazine ethyl sulfate (PES) was added. Under normal (non cytotoxic) conditions, PES can enter the cells, accept electrons from metabolic processes and convert tetrazolium into formazan, a purple dye. This was incubated for 4 hours at 37°C. The absorbance was read at 490 nm using a microplate reader. Higher absorbance (deeper purple and more formazan) indicates a higher number of metabolically active cells. The data was compiled into Excel for analysis.

2.9 PDMS Preparation and Plasma Treatment

PDMS was made using the Sylgard 184 commercial kit at a weight ratio of 10:1 (base to curing agent). PDMS molds were made by carefully lining small Petri dishes with aluminum foil,

ensuring to not rip or pierce the foil to prevent leakage. In a weigh boat, 18 grams of PDMS base (for about 8 Petri dishes filled halfway) and 1.8 grams of the curing agent (10:1 ratio) were mixed vigorously. The mixture was poured into the molds and large bubbles were removed from the surface of the PDMS mixture by blowing air from a pipette close to the surface. The molds were put into an oven at 60℃ and left overnight. Once cured, the aluminum foil was removed and the PDMS was either plasma-treated or not (controls). Plasma treatment was done with a corona plasma treater wand (Model BD-20) from Electro-Technic Products Inc. This was done by turning on the wand and letting it warm up for approximately one minute. Then, ensuring plasma is directed towards the PDMS, a slow sweeping motion was used to completely cover the surface of the PDMS for one minute. Once the plasma treatment was completed, microgels were added to either cover the surface or completely submerge the PDMS. The PDMS samples were put back into the oven at 60℃ overnight to dry.

2.10 Visual Tests for Microgel-PDMS Binding

2.10.1 Bromophenol Blue of Microgel-coated PDMS

Binding was assessed after different drying times (1 day, 2 days, 3 days). Visual observations of microgel binding were completed using bromophenol blue (BPB), a dye that changes to blue in the presence of QACs. The PDMS samples were removed from the oven and rinsed thoroughly three times with MiQ water to ensure no unbounded microgels were present. Then BPB was added to submerge the samples for five minutes. The samples were then thoroughly rinsed three times with MiQ to remove any residual BPB and microgels. Finally, any samples with QACs bound to the PDMS (and thus microgels) left a blue residue from BPB binding to QACs and qualitatively showed microgel binding to the PDMS.

2.10.2 Atomic Force Microscopy (AFM) of microgel-coated PDMS

Once the PDMS was cured it was rinsed thoroughly with MiQ water five times to remove any impurities. Then, the experimental sample of PDMS was plasma-treated for 45 seconds and the control sample was not plasma-treated. Immediately after the plasma treatment, the surface of the PDMS was covered in microgels and left in the oven at 60℃ overnight. The next day, both samples were rinsed five times and dried using pressurized air for five minutes. The samples were cut into squares of 5x5 mm ensuring to not touch or alter the surface of the PDMS. The samples were prepared for AFM by attaching them to microscope slides using double-sided tape. AFM was completed using a FastScan AFM microscope by Bruker. Images were observed and differences in morphology indicated if microgel coatings were present.

2.10.3 Scanning Electron Microscopy (SEM) of microgel-coated PDMS

Once the PDMS was cured, it was rinsed thoroughly with MiQ water five times to remove any impurities. The control sample was not plasma-treated or coated with microgels. The experimental samples were plasma treated, coated with microgels, and placed in the oven at 60℃ overnight. The next day, the samples were cut into 1x1 cm squares and placed onto pin mount sample holder for SEM. The samples were stuck to the sample holders using double sided tape. The samples were then sputtered with gold to prevent charging the sample and to the increase signal-to-noise ratio. The samples were then put into the SEM microscope and images were taken with a scan speed of 6 and magnifications of 100X, 500X, 1,000X, 5,000X, and 25,000X.

2.11 Microgel-coated PDMS Antibacterial Tests

The antibacterial properties of the microgel coated PDMS was assessed using a modified method from the American Society for Testing and Materials (ASTM) standard E2180 (Knobloch

et al., 2017). First, a starter plate was made by putting 10 µL of the stock *Staphylococcus aureus* on a petri dish with LB agar and streaking with a pipette tip. Similarly to the previous antibacterial assay, a 10^6 CFU/mL stock solution of *S. aureus* was obtained. For this study, four PDMS samples were uncoated, four were plasma-treated and coated with microgels, and four were plasma-treated, coated with microgels, and vortexed for one minute to mimic a cleaning procedure. The PDMS samples were put into 12-well plates and distilled water was added to adjacent wells to prevent desiccation. 20 µL of the 10^6 CFU/mL stock was placed in the centre of each PDMS sample and put into the incubator to grow overnight. The next day, 1980 µL of LB broth was put into a falcon tube, along with the PDMS for each treatment. These was vortexed for 30 seconds, sonicated for 30 seconds, and vortexed again for 30 seconds to dilute and suspend any bacteria on the surface. The solutions were serially diluted, plated on agar plates, then put into the incubator at 37 °C and left to grow overnight. The next day, the number of colonies were counted, and the data was inputted into Excel for analysis.

2.12 Microgel-coated PDMS Binding Stability

To visually observe if the microgel-PDMS bond is stable, four PDMS samples were plasma treated, coated with microgels, and left in the oven at 60°C overnight. The next day, the samples were rinsed thoroughly three times. BPB was added to two of the samples and let sit for five minutes. The other two samples were vortexed for 30 seconds and then BPB was added to their surface and let sit for five minutes. After five minutes, all samples were rinsed thoroughly three times. Any residual blue qualitatively indicates the microgels have bound to the PDMS surface.

3. Results

3.1 LCST of POHQ and POA

First, a corrected absorbance was obtained by subtracting the absorbance of MiQ (control) from the sample absorbance. Transmittance was calculated by the formula: $T = 10^A$, where T is the transmittance and A is the absorbance. This was normalized by dividing all transmittance values by the maximum transmittance for the sample. The temperature associated with 95% transmittance after the maximum transmittance (a value of 0.95 for the normalized transmittance) was considered to be the LCST. The lower the transmittance, the less miscible the polymer is in the solution. The normalized transmittance with increases in temperature in MiQ can be seen in Figure 6.

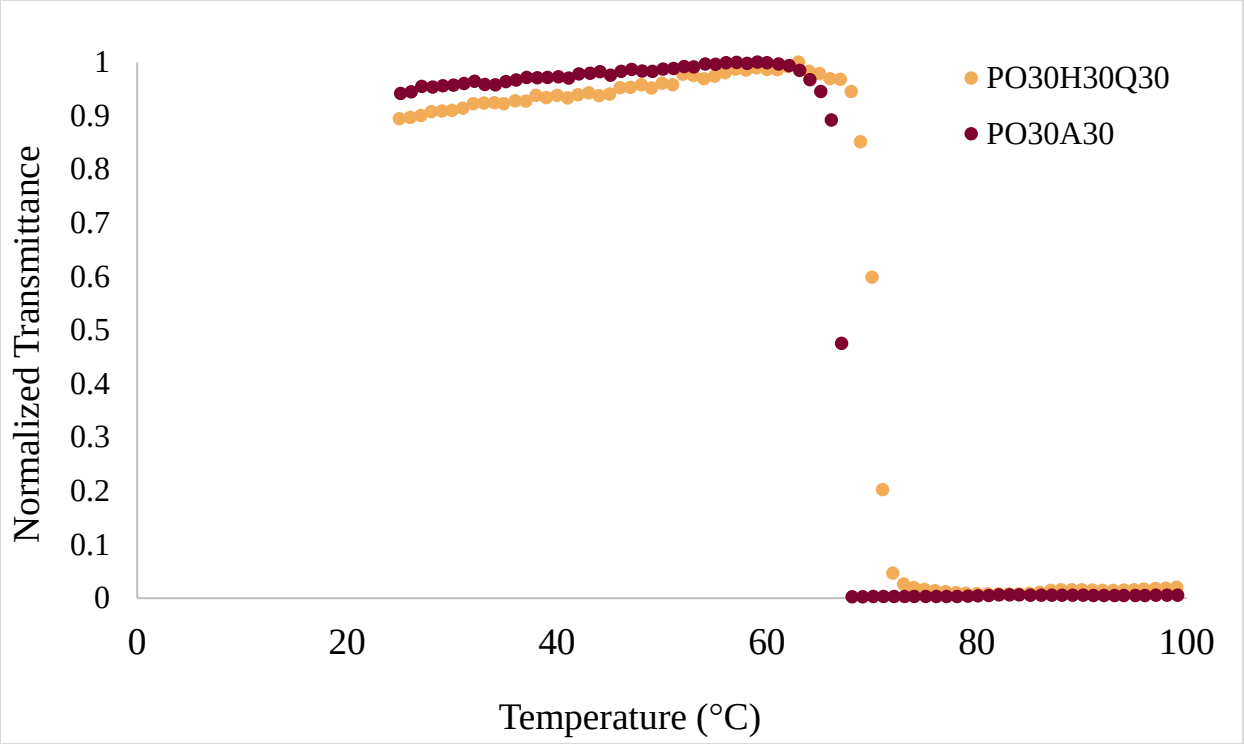

Figure 6. Normalized transmittance of POHQ and POA from 25 to 99℃ in MiQ. The orange dots represent PO30H30Q30, and the red dots represent PO30A30. A lower transmittance means the polymers are less miscible in the solution, meaning they are becoming immiscible. The LCST was determined to be the temperature at 95% after the maximum normalized transmittance.

The LCST of $PO_{30}H_{30}Q_{30}$ was determined to be 67.52℃ and the LCST of $PO_{30}A_{30}$ was determined to be 65.02 ℃ in MiQ. Figure 7 shows a normalized transmittance graph for the polymers in PBS.

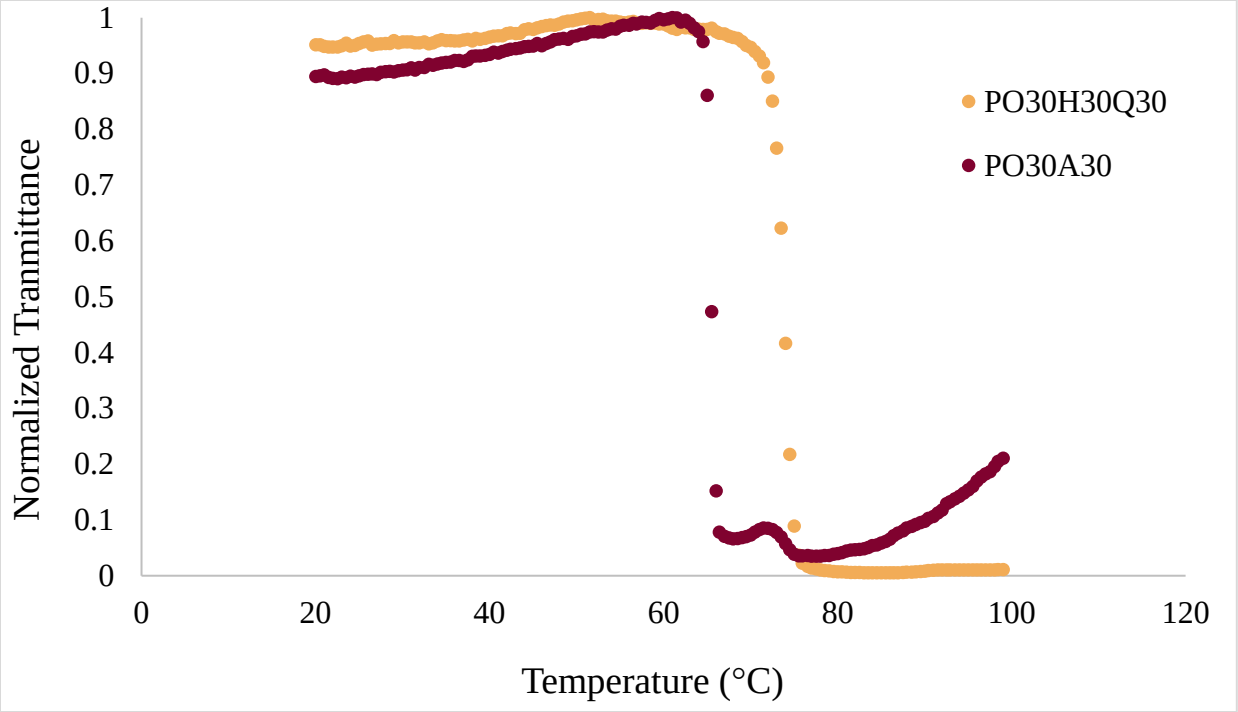

Figure 7. Normalized transmittance of POHQ and POA from 25 to 99℃ in PBS. The orange dots represent $PO_{30}H_{30}Q_{30}$, and the red dots represent $PO_{30}A_{30}$. A lower transmittance means the polymers are less miscible in the solution. The LCST was determined to be the temperature at 95% after the maximum normalized transmittance.

The LCST of $PO_{30}H_{30}Q_{30}$ was determined to be 69.52℃ and the LCST of $PO_{30}A_{30}$ was determined to be 64.53 ℃ in PBS. These LCST values were considered when synthesizing the microgels. A temperature of 85 ℃ was chosen as the ideal temperature because lower temperatures caused more aggregation of the polymers and increased polydispersity of the particles.

3.2 Microgel Stability

Microgel stability was observed to indicate aggregation and degradation of the microgels, in the context of storage. Microgel stability was assessed in MiQ and PBS, both showing stability over time. Figure 8 shows the stability of the microgels in MiQ over a 20-day period. The threshold for monodispersed microgels was determined to be 0.2 PDI units.

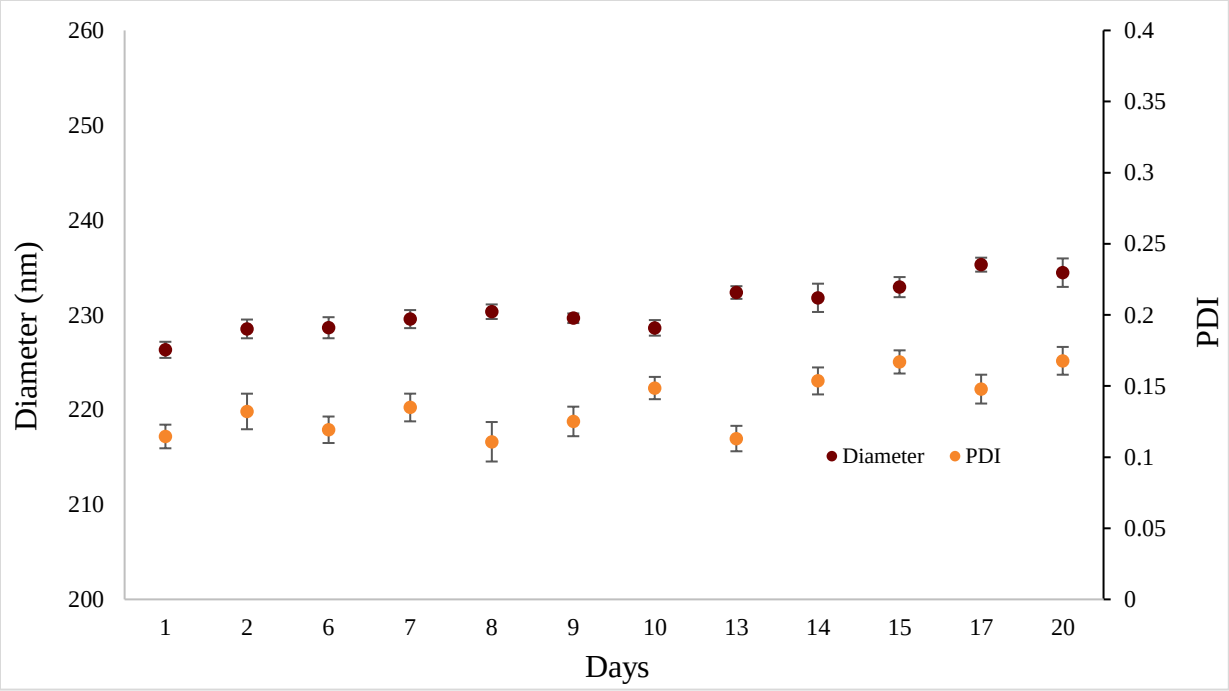

Figure 8. The average stability of microgels over a three-week period in MiQ. The horizontal axis shows the number of days, the left vertical axis shows the average diameter of the microgels, and the right vertical axis shows the PDI (polydispersity index). The red dots represent the diameter, and the orange dots represent the PDI. These data were obtained using DLS, the average of 6 collections per session are plotted and error bars represent the standard error.

Figure 8 shows that the diameter varies by an average of 9 nm, which indicates that the microgel size is consistent over the three-week period. The PDI values vary by an average of 0.057. This indicates that the dispersity is very consistent over time, meaning the microgels are highly monodispersed, even weeks after synthesis. Both results indicate that the microgels do not degrade or aggregate together for at least 3 weeks after their synthesis, when stored in MiQ.

Microgel stability was assessed in PBS to observe biologically relevant stability levels. Figure 9 shows the stability of microgels in PBS over a 20-day period.

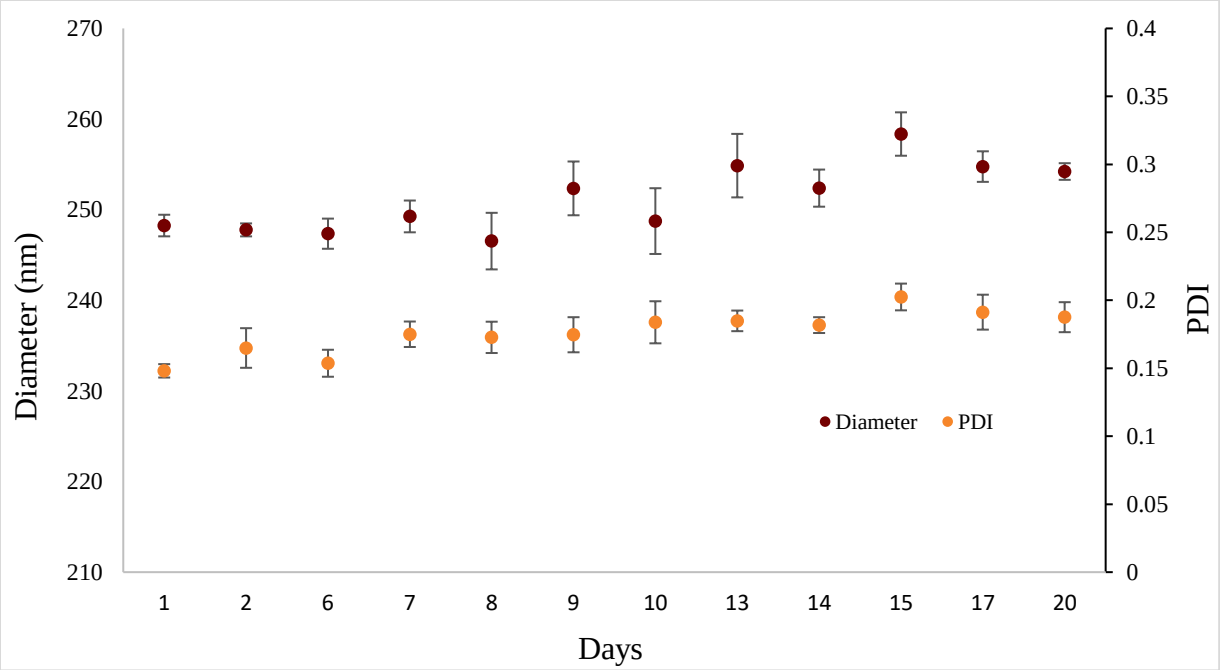

Figure 9. The average stability of microgels over a three-week period in PBS. The horizontal axis shows the number of days, the left vertical axis shows the average diameter of the microgels, and the right vertical axis shows the PDI. The red dots represent the diameter, and the orange dots represent the PDI. These data were obtained using DLS, the average of 6 collections per session are plotted and error bars represent the standard error.

Figure 9 shows that the diameter of microgels vary by an average of 8 nm, indicating their size is very consistent over time. Their PDI values vary by an average of 0.054. This indicates that the microgels are do not degrade or aggregate over this 3-week period. However, the average PDI value for day 15 shows a PDI of 0.202, which is slightly higher than our accepted monodispersed threshold. This is most likely because the PDI values and diameters of microgels in PBS are slightly higher than those in MiQ. This indicates that making microgels in PBS causes them to be slightly larger and more polydisperse. That being said, the diameter and PDI are very consistent over time, indicating the microgels are stable for at least three weeks when synthesized and stored in MiQ and PBS.

3.3 Microgel Antibacterial Properties

Antimicrobial tests were used to determine the killing efficacy of the microgels against biofilm forming bacteria. Antimicrobial tests were first completed with *S. aureus*, a Gram-positive biofilm-forming bacteria, and its growth was recorded using OD600 absorbance measurements. The results can be observed in Figure 10.

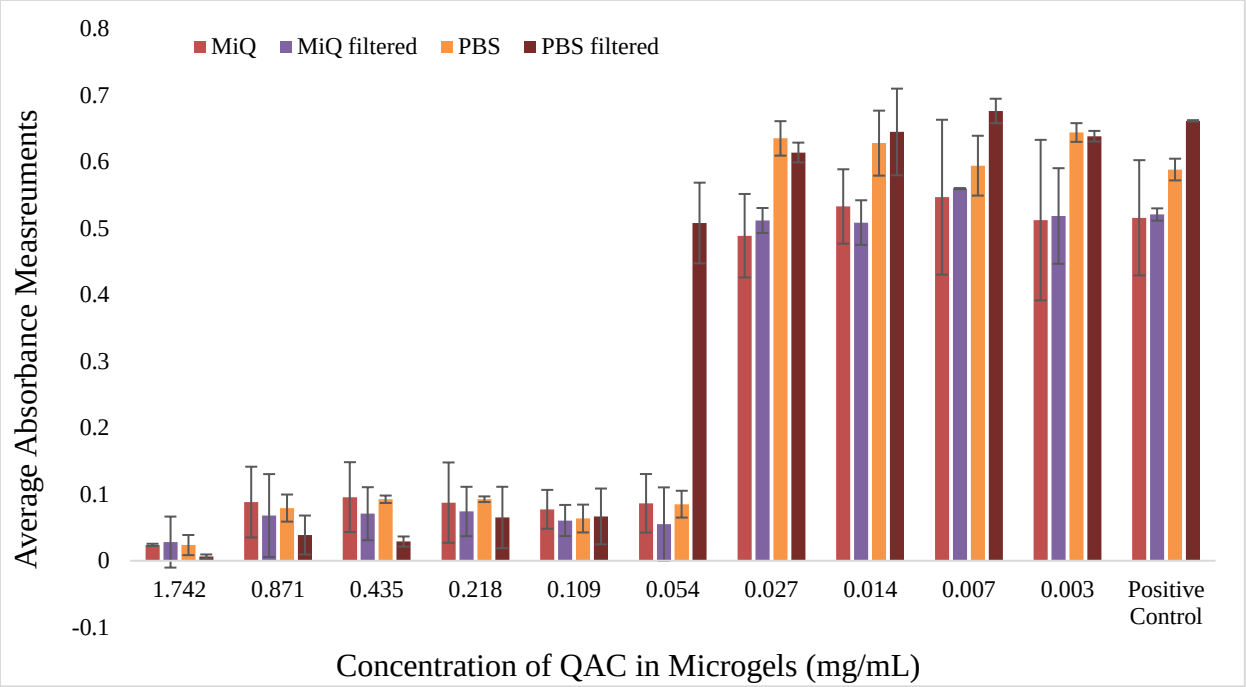

Figure 10. The average absorbance of OD600 measurements for S. aureus for varying concentrations of QACs. The horizontal axis represents the concentration of QACs (in mg/mL) for each sample obtained by serial dilutions. The vertical axis shows the average absorbance of light for each condition. Dark red bars and orange bars represent PBS filtered and unfiltered conditions, respectively. The light purple bars and red bars represent the MiQ filtered and unfiltered conditions, respectively. Lower absorbance values are directly proportional to bacterial inhibition.

Figure 10 shows how the average absorbance is changed with varying concentrations of QACs in the samples. For concentrations up to 0.054 (32 times dilution), average absorbance values are less than 0.1 (except for PBS filtered), indicating that the microgels effectively killed *S.*

aureus even in lower concentrations. Log reductions were calculated using the formula: $\log_{10}\left(\frac{A}{B}\right)$, where A is the average absorbance for the first 4 dilutions in filtered MiQ and PBS (1x, 2x, 4x, and 8x), and B is the absorbance of the positive control. This calculation showed a log reduction of 9.54, or 99.99999997% killing efficacy. This indicates that the microgels are very effective against *S. aureus*, indicating full disinfection, or log reduction of 6 or higher (Altapure, 2024).

To observe efficacy against gram-negative biofilm forming bacteria, we completed the same tests with *P. aeruginosa*. Figure 11 shows the results for this test.

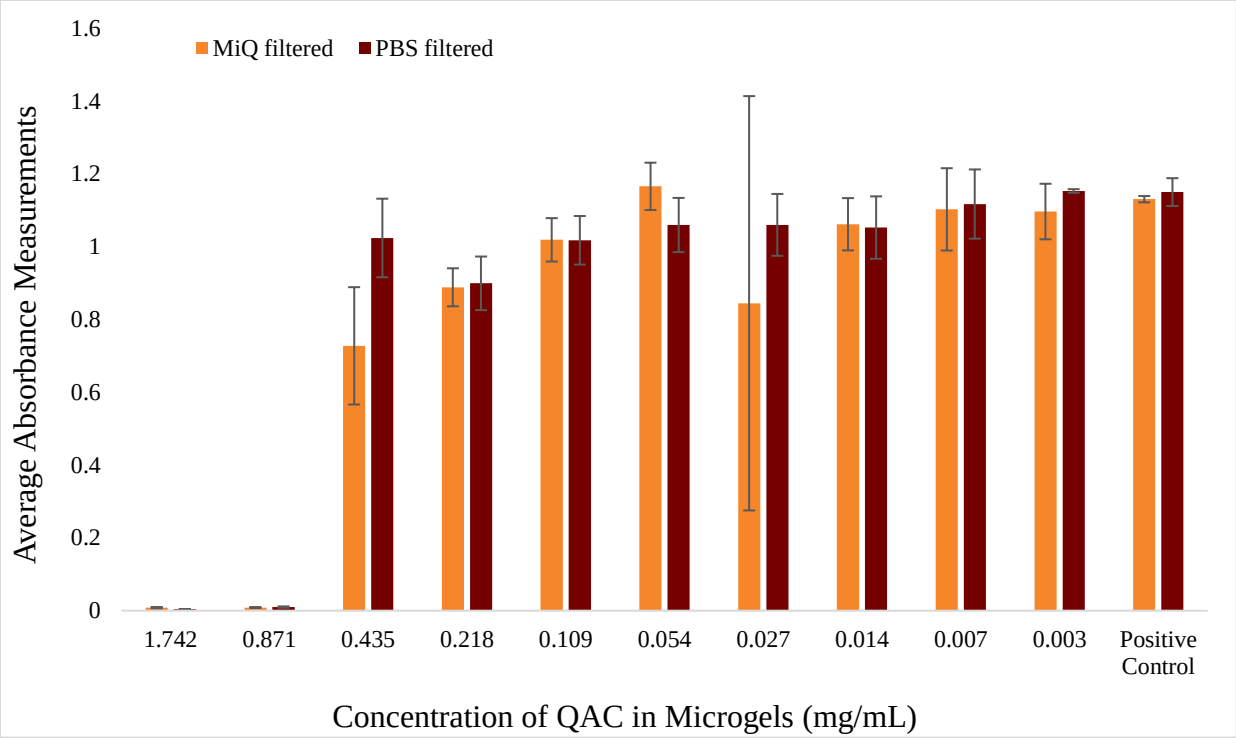

Figure 11. The average absorbance of OD600 measurements for P. aeruginosa for varying concentrations of QACs. The horizontal axis represents the concentration of QACs (in mg/mL) for each sample obtained by serial dilutions. The vertical axis shows the average absorbance of light for each condition. Dark red bars and orange bars represent PBS filtered and MiQ filtered conditions, respectively. Lower absorbance values are directly proportional to bacterial inhibition.

Figure 11 shows the average absorbance of light for varying concentrations of QACs. For concentrations up to 0.871 (2 times dilution), the absorbance values were nearly 0, indicating effective killing of *P. aeruginosa*. Log reductions were calculated in the same way as for *S. aureus*, comparing absorbance of the 2 times dilution to the positive control. These calculations showed an 8.5 log reduction or 99.9999997% killing efficacy. This indicates that the QAC functionalized microgels are highly effective against *P. aeruginosa*, showing complete disinfection of the samples. Overall, the microgels were observed to show full disinfection of the *S. aureus* and *P. aeruginosa* (log reduction higher than 6). This indicates that the microgels could be a successful disinfectant surface coating.

3.4 Microgel Cytotoxicity

Cytotoxicity of the microgels was observed to indicate the likelihood for their *in vivo* use. Cytotoxicity was determined using an MTS assay with 3T3 murine fibroblasts. Metabolic activity of the cells was observed as the level of formazan converted from tetrazolium, indicated by higher absorbance from the 490 nm light. Results from this test can be observed in Figure 12.

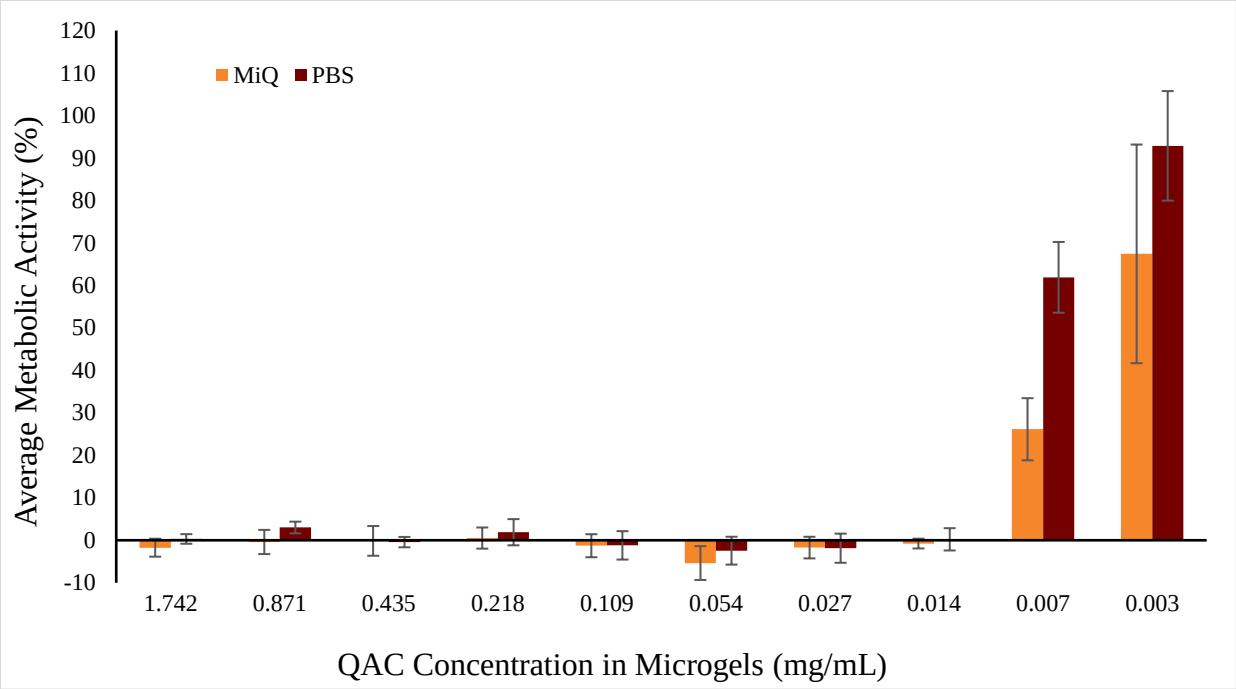

Figure 12. The average metabolic activity of 3T3 murine fibroblasts with varying concentrations of QAC-functionalized microgels. The horizontal axis shows the QAC concentration for each condition, obtained by serial dilutions. The vertical axis shows the metabolic activity which is directly proportional to formazan absorbance at 490 nm. The red and orange bars represent filtered PBS and MiQ, respectively.

In Figure 12, the first 8 (1.742 to 0.014 mg/mL) dilutions have an extremely low average rate of metabolic activity (roughly 0%). This indicates that the microgels are extremely cytotoxic against mammalian cells, even at low concentrations. Metabolic activity increased to roughly 26% and 61% in MiQ and PBS (respectively) for the QAC concentration of 0.007 mg/mL, and to

roughly 67% and 93% in MiQ and PBS (respectively) for the QAC concentration of 0.003 mg/mL. It is important to note that the concentrations of effective bacterial reduction (0.054 and above for *S. aureus*) demonstrate high cytotoxicity.

3.5 Qualitative Tests for Microgel-PDMS Binding

3.5.1 Visual Test of microgel-PDMS binding using BPB

The first qualitative test used to visualize microgel-PDMS binding was using BPB. This dye turns blue in the presence of QACs, which are the biocidal components of the microgels. Since the samples were rinsed thoroughly before and after BPB addition, any bound microgels should show a residual blue colour that is attached to the PDMS surface. This result can be seen in Figure 13.

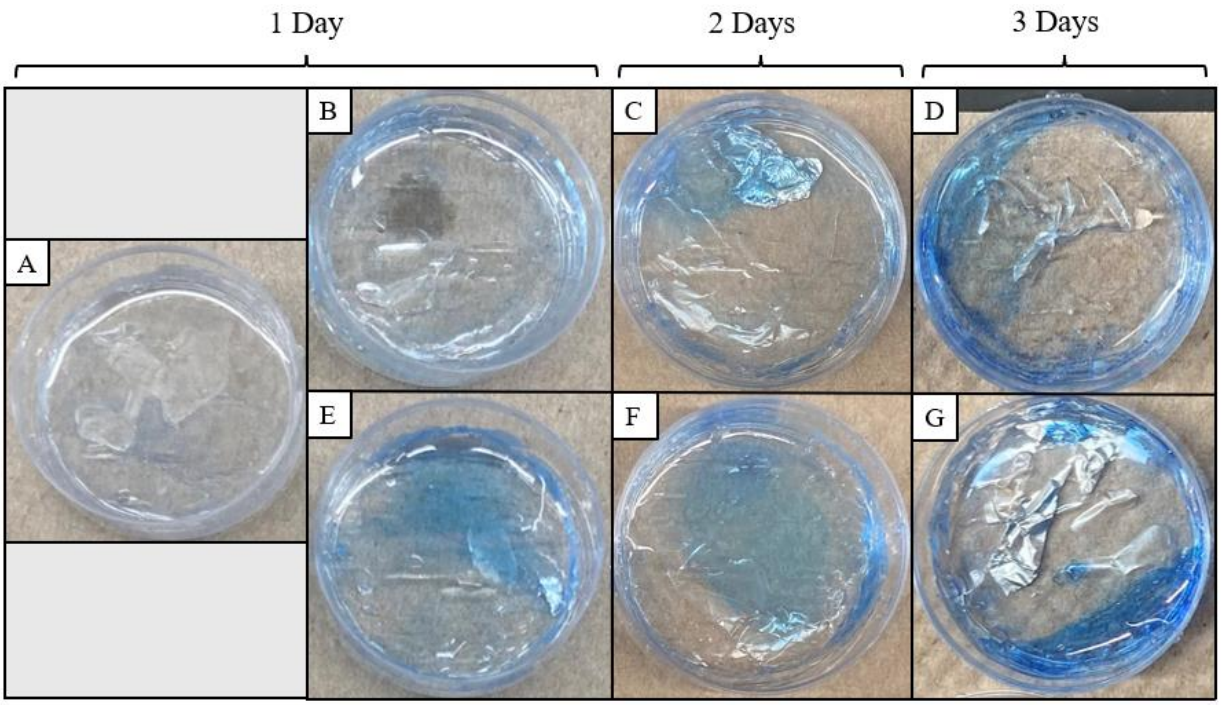

Figure 13. Images of BPB addition to microgel-coated PDMS. The figure is separated into 3 sections, 1 day post microgel treatment, 2 days post microgel treatment, and 3 days post microgel treatment. Panel A is the negative control, showing untreated PDMS one day post microgel treatment. The PDMS in panels B, C, and D were submerged with microgels and panels E, F, and G were coated on their surfaces.

Figure 13 shows images of various microgel-coated PDMS samples. Panel A is the negative control, showing no residual BPB, indicating no microgels (or very few) were bound. Panels B, C, and D were submerged with microgels. These conditions show some residual BPB, particularly with more days in the oven. This indicates that microgels were able to bind to PDMS after the plasma treatment when the PDMS is submerged with the microgel solution. Panels E, F, and G show PDMS that was surface coated (not submerged) with microgels. These conditions show more residual BPB on their surface, indicating the microgels bind better when coating the surface and not submerging the whole sample. This is most likely due to the surface tension of the MiQ microgel solution. Only the surface of the PDMS was treated with oxygen plasma, thus, as the microgel solution dries in the oven, it is possible that the solution was redirected to under the

PDMS itself due to surface tension. This may be the reason the surface does not have as much residual BPB compared to the surface-coated conditions. The residual BPB becomes more concentrated as the number of days in the oven increases. These results indicate that the microgels bind better over time in a heated environment.

3.5.2 AFM of Microgel-coated PDMS

The second qualitative method to observe microgel binding was AFM. Figure 14 shows AFM images for untreated, uncoated PDMS.

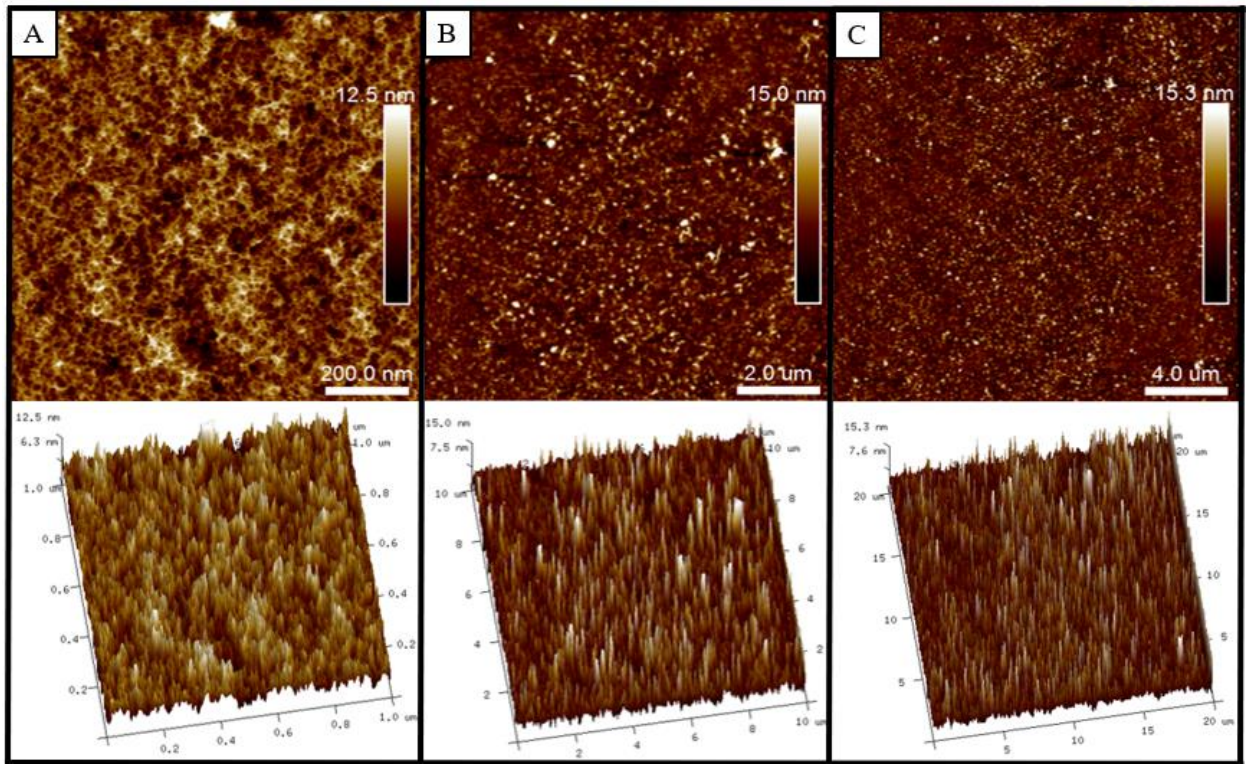

Figure 14. Untreated PDMS AFM images. Panel A shows a 1x1 µm two-dimensional image (top) and three-dimensional image (bottom) of untreated PDMS. Panels B and C show the same but for images of size 10x10 µm and 20x20 µm, respectively. Lighter colours represent taller morphology.

Figure 14 shows the structure of uncoated PDMS, highlighting slight changes in morphology based on colour brightness. In panel A, crosslinking of PDMS polymers are observed

around air bubbles. In panels B and C, it is possible to see larger aggregations of PDMS polymers, highlighted in lighter colours indicating taller morphologies. Overall, uncoated PDMS is smooth and flat, with height variations of roughly 15 nm.

The next step was to observe how the morphologies differ upon coating with microgels. These results can be observed in Figure 15.

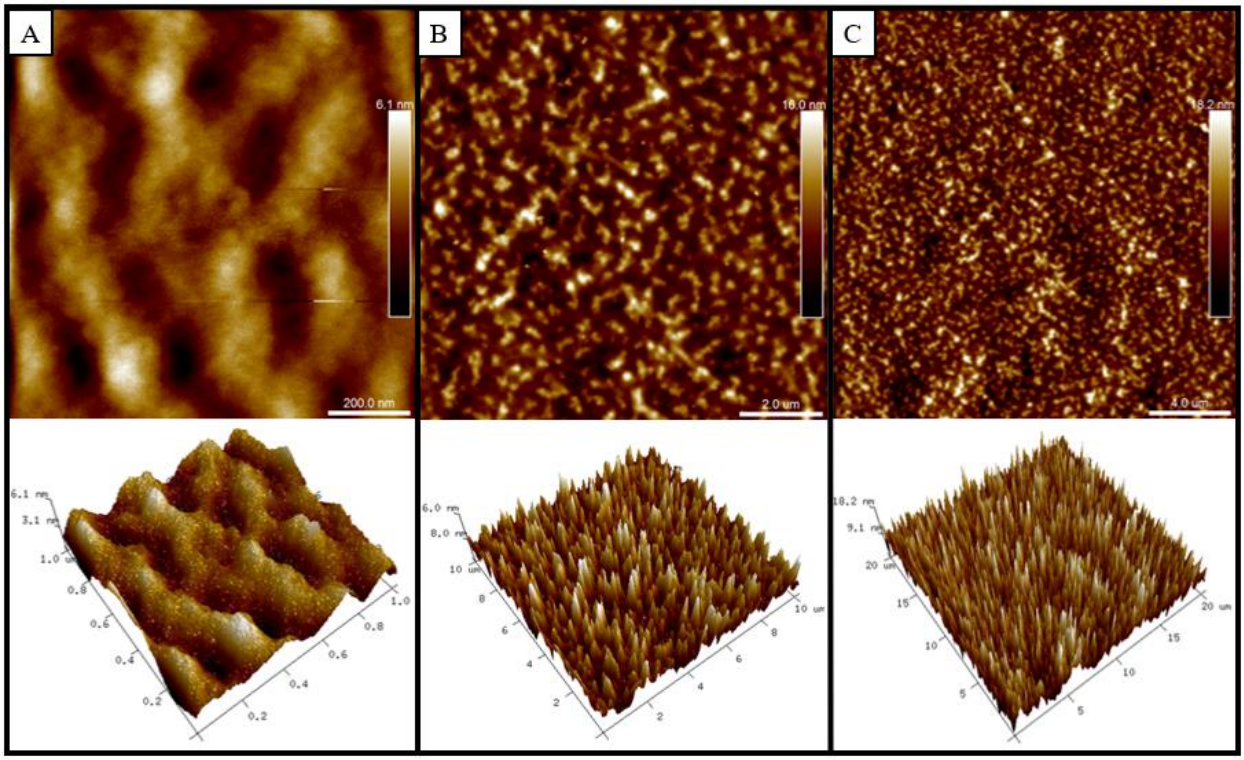

Figure 15. Microgel-coated PDMS AFM images. Panel A shows a two-dimensional image (top) and three-dimensional image (bottom) of a 1x1 µm area of microgel-coated PDMS. Panels B and C show the same but for images of size 10x10 µm and 20x20 µm, respectively. Lighter colours represent taller morphology.

Figure 15 shows vastly different surface morphology when compared to Figure 14. For panel A of Figure 15, the surface morphology is smooth and wave-like. Its height variations are roughly 6.1 nm, indicating a smoother surface than the uncoated PDMS. Panels B and C show large aggregations of particles on the PDMS surface, shown as lighter clusters. The distribution of

the aggregations is also fairly homogenous. Overall, this likely shows that microgels were able to successfully coat the surface of PDMS, but qualitative experiments should be used to confirm this.

While the microgels were successfully coat the PDMS, there were several patterns that emerged throughout the drying process. Figure 16 shows the wave-like patterns observed by taking images on the same PDMS sample from Figure 15.

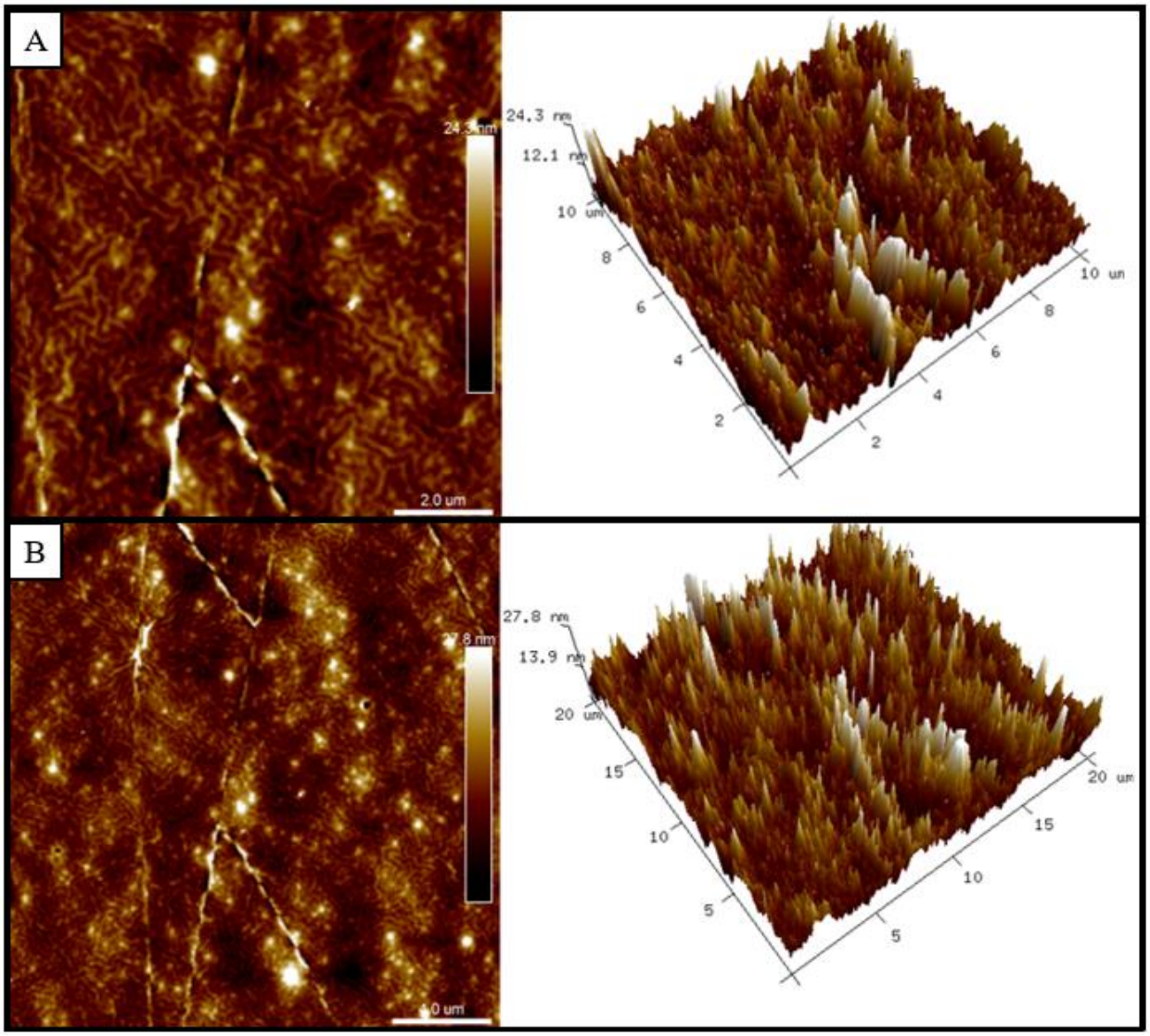

Figure 16. Alternate microgel-coated PDMS AFM images. Panel A shows a two-dimensional image (left) and a three-dimensional image (right) of a 10x10 µm area of microgel-coated PDMS. Panel B shows the same but for a 20x20 µm area of microgel-coated PDMS. This sample is the same sample as Figure 13 but at a different location.

Figure 16 shows wave-like aggregations of microgels all over the PDMS surface. Larger aggregations of microgels can be observed along the cracks in the PDMS surface. These patterns are likely due to differing drying conditions. Wave-like patterns are likely to be produced with slower drying conditions (Lee et al., 2022). This could allow for electrostatic interactions between microgels within the solution before fully drying. This is also supported by the fact that the

microgels are supposedly homogenously distributed over the surface of the PDMS. This indicates that microgels did not submit to surface tension forces while drying, or else they would likely aggregate into larger clusters of microgels.

Another pattern observed on the PDMS surface as a result of microgel coating is seen in Figure 17.

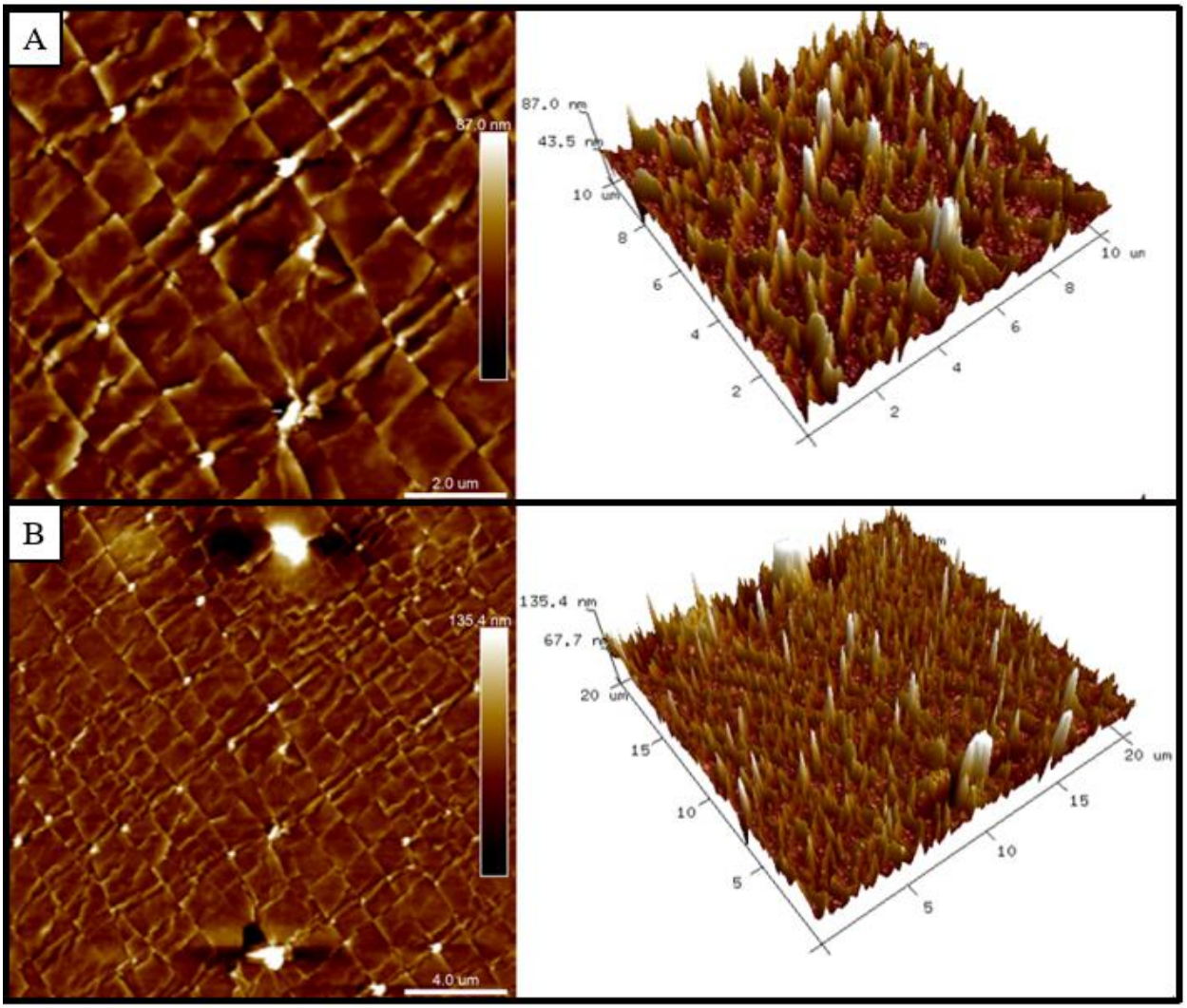

Figure 17. Alternate microgel-coated PDMS AFM images. Panel A shows a two-dimensional image (left) and a three-dimensional image (right) of a 10x10 µm area of microgel-coated PDMS. Panel B shows the same but for a 20x20 µm area of microgel-coated PDMS. This sample was taken from a different PDMS sample, different from previous figures.

Figure 17 shows a square lattice-like pattern all over the surface of the PDMS. There are also larger aggregations of microgels, shown as the white peaks in the AFM images. These have a maximum diameter of 138 nm, which is over 100 nm larger than those on any other PDMS sample. These patterns are likely from fast drying conditions, or a thinner film of microgel suspension on

the PDMS surface (Yang et al., 2016). This shows that the coating of microgels should be even on PDMS surfaces to maximize its surface area and applications.

3.5.3 SEM of Microgel-coated PDMS

The third qualitative method to observe microgel binding was scanning electron microscopy. Figure 18 shows the images for uncoated, coated, and coated and vortexed PDMS.

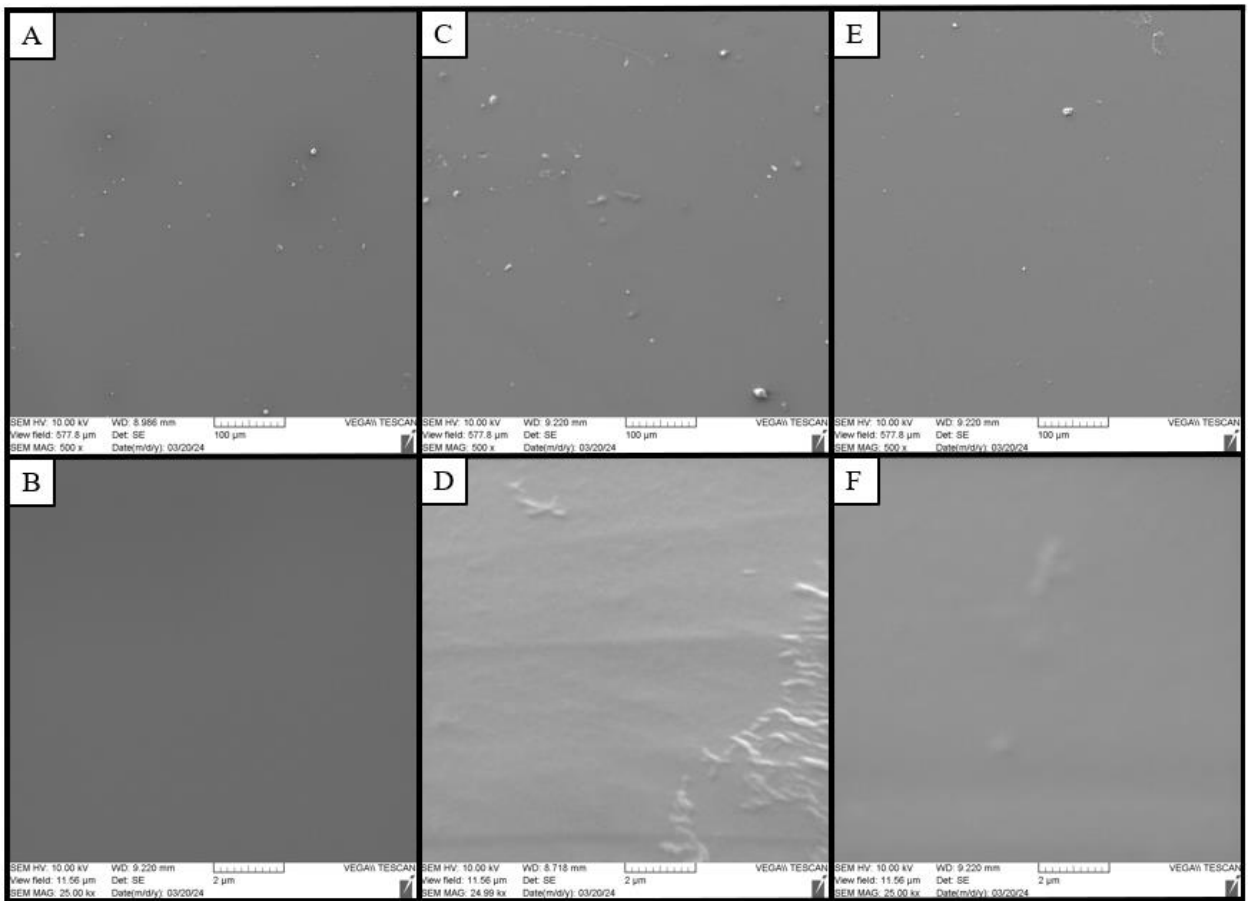

Figure 18. Scanning electron microscopy of PDMS samples. Panels A and B show an uncoated PDMS sample, C and D show a coated sample, and E and F show a coated and vortexed sample. Panels A, C and E (top row) are at a 500X magnification, and panels B, D, and F (bottom row) are at 25,000X magnification.

Panels A and B of Figure 18 show a relatively smooth surface. Panel A (500X magnification) has some small particles spread across the PDMS surface, which is likely dust or

dirt. The particles are too large to be considered microgels. Panel B (25,000X magnification) shows a smooth surface with no aggregations. Panel C shows a coated surface of PDMS at a 500X magnification. This surface has more particles spread across its surface; however, these are likely not microgel aggregations. Panel D shows the same but at a 25,000X magnification. This surface has some wave-like patterns along the surface. The diameter is consistent with that estimated from AFM, however, that does not indicate that microgels have bound to its surface. It is difficult to distinguish if microgels are present or not. Panel E shows a coated and vortex PDMS sample at a 500X magnification. This surface is similar to the uncoated PDMS sample in that there are very few particles across its surface, but they are likely to be dirt or dust. These particles are much too large to be deemed with certainty to be microgels. Panel F shows the vortexed sample at a 25,000X magnification. This sample is smooth but there is evidence of slight columnar aggregations on the PDMS surface. Similarly to panel D, it is not possible to determine what these structures are; thus, it does not indicate microgel binding. Overall, SEM was inconclusive to determine if the microgels bound to the surface of PDMS.

3.6 Microgel-coated PDMS Antibacterial Properties

Next, the antimicrobial properties of microgel-coated PDMS were assessed. Three conditions were assessed, uncoated PDMS (positive control), plasma treated and coated with microgels, and the plasma-treated, coated with microgels and vortexed to assess stability. Figure 19 shows the results of the contact killing for *S. aureus*.

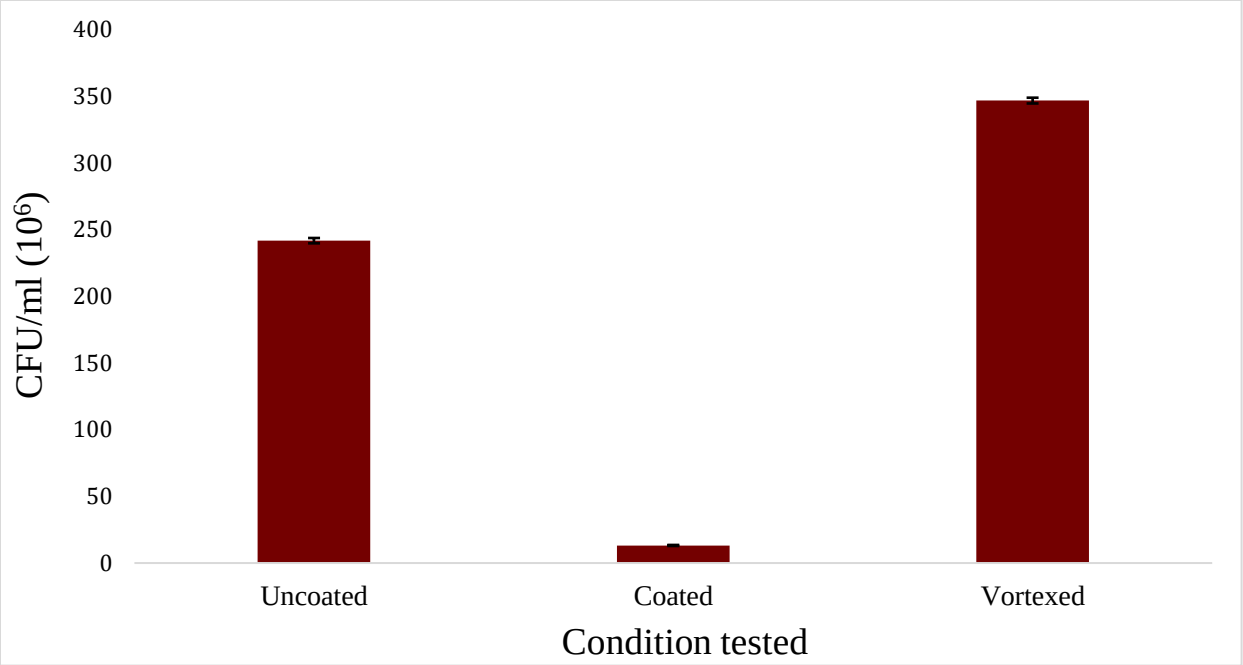

Figure 19. The average CFUs for microgel-coated PDMS. The uncoated sample was simply PDMS, the coated sample was plasma-treated and coated with microgels, and the vortexed sample was plasma-treated, coated with microgels and vortexed for 30 seconds before bacterial deposition.

Figure 19 shows a 1.32 log reduction between the uncoated and coated samples, which is equivalent to a 95% reduction in bacterial growth. This indicates that the microgels were able to sanitize the surface of the PDMS. However, the vortexed sample showed a 42% increase of bacterial growth.

3.7 Visual BPB Test for Microgel-PDMS Binding Stability

Due to the increase in bacterial growth from the vortexed condition in the previous result (Figure 19), a visual stability test was performed to observe microgel-PDMS bond stability. Four PDMS samples were coated with microgels, and two of these were vortexed before BPB addition. Figure 20 shows the images of the PDMS for this test.

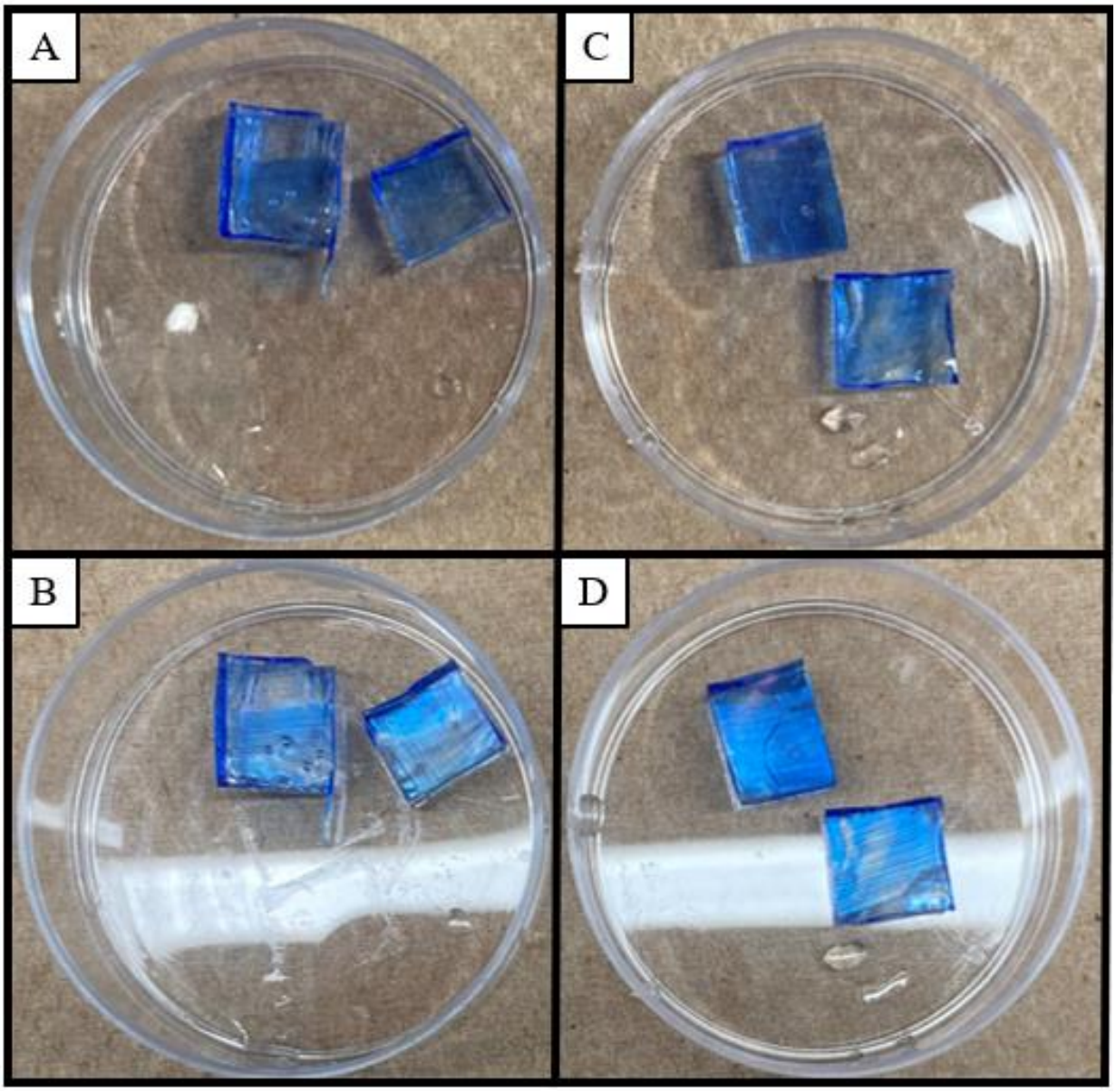

Figure 20. Microgel coated PDMS bond stability with BPB. Panels A and B show the vortexed condition, while panels C and D show the non-vortexed condition. Panels B and D show the same samples as A and C respectively, however different lighting was used to highlight the residual BPB.

Panels A and B show the vortexed samples and panels C and D show the non-vortexed samples. Panels B and D show the same samples as A and C but with different lighting. The samples in panels A and B should show much less residual BPB after vortexing, however, there is a remarkably similar amount of BPB, compared to the non-vortexed condition. Panel B shows a

slightly more transparent samples than panel D, indicating the some of the microgels did get removed during the treatment. However, since this test is simply qualitative, it does not indicate the number of microgels on the surface of the PDMS. Thus, the visual BPB stability test is inconclusive to determine of microgel-PDMS bonds are stable.

4. Discussion

The LCST of $PO_{30}H_{30}Q_{30}$ and $PO_{30}A_{30}$ were determined to be below 70°C. Thus, a temperature of 85°C was used to self-assemble the microgels. Lower temperatures did not allow the polymers to aggregate into microgels. In Figure 7, (PBS condition) the POA polymer was observed to start gelling once the cuvette removed from the UV-Vis equipment. This was likely due to the interactions with the salts in the PBS but does not affect the results for the LCST. Thus, it is not a major concern.

The microgels were observed to be highly stable over a three-week period in both MiQ and PBS. This indicates that the microgels can be stored at room temperature for at least three weeks without degrading or aggregating in these solvents. Microgel diameter values for MiQ and PBS only varied on an average of 9 nm and 8 nm respectively, showing minor variation. Furthermore, the PDI values stayed below 0.2 for all measurements, except for one in PBS (0.202 on day 15), indicating the microgels do not aggregate or dissolve in the solutions. While the microgels are stable over a three-week period in ambient temperatures, their stability should be checked for a larger amount of time (months or years) to observe long-term degradation, especially in different temperatures. Some studies have shown greater stability of PNIPAM microgels when stored at temperatures below 4°C (Li et al., 2021), however, there is a lack of research for POEGMA microgels.

Upon testing for antimicrobial properties, the QAC-functionalized microgels were found to completely disinfect bacterial colonies in LB media. This is indicated by a log reduction of 6 or higher (Altapure, 2024), which was attained by tests against *S. aureus* (9.56 log reduction) and *P. aeruginosa* (8.5 log reduction). This indicates that the microgels are extremely efficient as antimicrobial agents on their own, specifically at higher concentrations. For example, ethanol sprays in hospital applications have log reductions against *S, aureus* and *P. aeruginosa* of between 3 to 6 for both bacteria (Costa et al., 2017; Ribeiro et al., 2015). Thus, at the very least, these microgels could be used to disinfect medical surfaces before surgical procedures and ensure a sterile environment is obtained.

For medical applications, the microgel cytotoxicity is a concern. When comparing Figure 12 (cytotoxicity) to Figures 10 and 11 (antibacterial graphs for *S. aureus* and *P. aeruginosa*), the microgels reduce the metabolic activity in 3T3 fibroblasts more effectively than they reduce bacterial growth. For example, in Figure 12, QAC concentrations as low as 0.014 mg/ml reduce metabolic activity to 0 (or less), whereas the microgels were able to effectively reduce bacterial growth for concentrations of QACs of 0.054 mg/ml or higher indicating these microgels as should not be used in medical applications. In other words, they are more cytotoxic than antibacterial. However, in the context of coating surfaces not intended to interact with cells for an extended period of time, cytotoxicity is not a major concern. For example, in food processing, these microgels could be used as a surface coating for machines or food preparation surfaces that use PDMS. These applications do not require the microgels to be non-toxic because they could be used to reduce biofilms on exposed parts. These may or may not be directly involved in food contact but washing them away or diluting them makes them safe for humans consumption (Camagay et al., 2024). At the very least, these microgels could be used as a surface disinfectant, which would

not need to be bound to PDMS. This could be used as a surface disinfectant which is then washed away to avoid cytotoxicity. This could even be applied to medical applications as long as the microgels are not directly interacting with living cells.

4.1 Qualitative Tests for Microgel Binding

While the BPB indicated that the microgels were in fact bound to the surface of the PDMS, this is simply a qualitative measure. However, certain properties could be theorized from this test. Figure 13 shows an uneven spread of microgels across the surface of the PDMS (patchy surfaces), and the submerged conditions showed much less microgel binding than the surface coated. This was slightly unexpected, however, there are a few explanations for this occurrence. The first is that the plasma treatment was not completed effectively for all samples. The BPB visual test was used as a proof-of-concept that the microgels could be bound to PDMS. However, initially the method of plasma-treating was not perfected, which may have led to human error. To ensure the even spread of plasma, the plasma coming from the wand must be directed towards the surface. It is possible that for some samples, the plasma was not evenly directed at all areas, which could explain why some areas are patchy. The second is that the surface tension of the microgels (in MiQ water) caused the liquid to be taken off the surface for submerged conditions and redirected to the bottom of the petri dish. Submerging the PDMS was only done until the solution was slightly above the PDMS surface. Once the liquid dried, the surface tension of the water could have directed the solution from the PDMS surface and on to the bottom of the petri dish. This was observed for certain samples during the coating process but was deemed to not be a major concern because the microgels should have created electrostatic bonds with the PDMS very quickly. Upon reflection, this may have been an important factor and should be considered for future research. The third

possibility could have been the improper coating of the surface of the PDMS. By not ensuring an excess of microgel solution is present, it is possible that different drying patterns can develop (Lee et al., 2022). Lee et al. (2022) showed that droplet size and its natural shape can affect how the microgels deposit along the surface. Notably, they showed that if a droplet contains a dip in the centre, while the outsides have a higher morphology, most of the microgels will deposit in the centre of the droplet as it dries. This is also known as Marangoni drying and could explain why the microgels were arranged in patches (Lee et al., 2022). Despite these variations, the microgels were observed to bind to PDMS with qualitative methods, indicating that a surface coating is feasible, but must be assessed further.

The differences in morphology were observed using AFM. Figures 14-17 show vastly different surface morphologies between microgel coated PDMS and uncoated PDMS (Figure 15). Since the samples were rinsed thoroughly five times for AFM preparation, it is fair to say that the microgels can coat the PDMS. Many different patterns were observed on the microgels during AFM. For example, Figure 15 shows a wave-like pattern on the 1x1 μm scale, but an even spread of particles on a 20x20 μm scale. Alternatively, Figure 15 showed wave-like aggregations of microgels across the whole surface of the PDMS. Figure 16 showed cracks across the surface and larger aggregations along the cracks, but also showed smooth morphology between them. Both the wave-like and cracked surfaces are likely due to differences in drying conditions. It is possible that slower drying conditions could have made the wave-like pattern observed in Figure 15 (Dieuzy et al., 2021). This could be because the surface of the sample was completely coated in microgels and drying occurred as the water evaporated. This would have allowed the microgels arrange themselves in wave-like patterns due to the intermolecular electrostatic interactions between the microgels. In other words, as the solvent evaporated, the microgels likely stayed in suspension but

arranged themselves in the wave pattern due to electrostatic interactions between the extra hydrazide groups present in the polymers. Dieuzy et al. (2021) showed something similar to this using a thick film (1-2 mm) of POEGMA microgels on glass. They found that a thicker suspension of microgels (with slower drying conditions) showed more linear and wave-like morphologies emerge. This is consistent with the observations from our surface-coated microgels.

A fast-drying condition is likely to yield the cracked surface with higher aggregations seen in Figure 17. This could be because the microgel solution did not completely cover the surface of the PDMS, or that it was a very thin coating. This is because the fast drying of the liquid would have caused some droplets to be stuck on the surface, specifically near the cracks due to surface tension. This would have caused more microgels to be suspended in the droplets before they completely dry and aggregate, which is consistent to Figure 17. Yang et al. (2016) showed comparable results to this, indicating that a thinner coating (or faster drying) showed evidence of shear and delamination as the solution dried. Thus, when the microgel solution was evaporating, it could have caused adjacent layers of the solution to be moved against each other, causing shearing. Since the microgel solution was not technically liquid but a suspension of solid-like particles, this shearing is a possibility and would be observed by very large aggregations of microgels along the cracks (Yang et al., 2016). These results indicate that the microgel solution should be evenly coated over the surface of the PDMS in order to get a well distributed sample. The drying patterns of POEGMA microgels on PDMS are intriguing but there is a severe lack of research into why they occur. Thus, the patterns should be considered in future research.

Unfortunately, SEM was not able to indicate if microgels bound to the surface of the PDMS. However, there are some indications that should be considered. The sample representing panel A from Figure 18 showed an uncoated sample of PDMS. Since this sample was simply rinsed

after PDMS curing, it makes sense that there are less dirt or dust particles on its surface. Conversely, panel C from Figure 18 shows a coated PDMS sample which was manipulated much more after curing. Thus, more unwanted dirt or dust particles were able to coat its surface. This likely overshadowed the evidence of microgel binding on its surface. That said, panel D showed some wave-like patterns, consistent with previous observations in AFM. These patterns could possibly be due to microgel aggregation; however, it is unlikely. Other than this wave-like pattern, no other aggregations of this form were found on the sample. This indicates that the microgels likely did not coat the PDMS properly, leading to inconclusive observations. Finally, panel E shows a sample that was vortexed, showing less particles on its surface compared to the unvortexed sample. This is most likely due to the mechanical forces of vortexing which could have caused dirt or dust particles to dislodge from the PDMS surface. Panel F shows slight columnar aggregations; however, the resolution is not excellent. Again, it is not possible to deduce if microgels have bound to the surface of the PDMS. Overall, this test indicates that there was likely a lot of error when coating the microgels to the surface of the PDMS because SEM resolution should be roughly 10 nm with an effective magnification of about 20,000X (Alberts et al., 2002). The microgels have average sizes of 230 nm, thus, they should have been clearly visible. In the future, careful preparation of the microgel coating, possibly through spin or blade coating could improve these results.

4.1.1 Microgel Binding Scheme

Based on the qualitative microgel binding tests and knowledge on the molecular composition of the sample PDMS and the microgels, the interaction between microgels and PDMS is likely due to electrostatic binding. There are leftover hydrazide groups in the microgels that could create hydrogen bonds with the hydroxyl groups on the PDMS from the plasma treatment.

Notably, the hydroxyl groups would likely interact with the acyl groups on the leftover hydrazides. The hypothetical arrangement is seen in Figure 21.

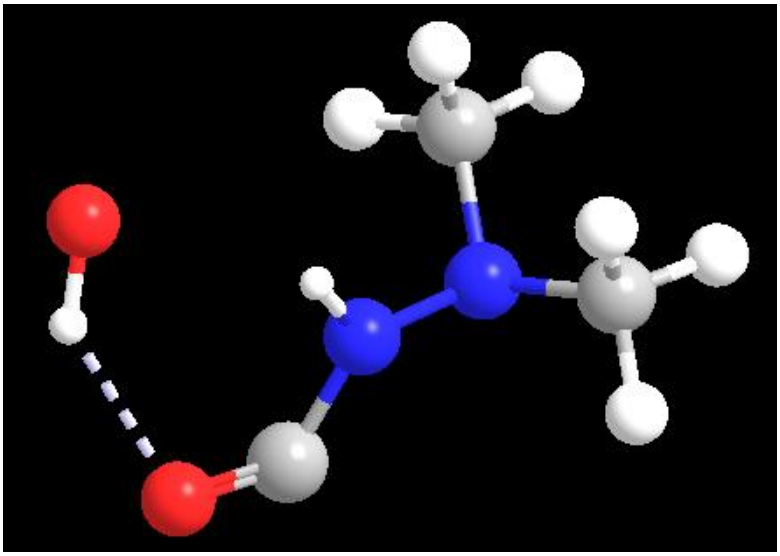

Figure 21. Image of the three-dimensional arrangement of a hydrazide and a hydroxyl group. The red atoms are oxygen, the blue atoms are nitrogen, the grey atoms are carbon, and the white atoms are hydrogen. The hydrazide group is on the right (with formula O=C-NH-N-(CH_3)) and the hydroxyl (OH) is seen on the left. The electrostatic interaction is seen by the dashed hydrogen bond between the acyl and hydroxyl groups. This schema was generated using ChemDraw 3D.

Figure 21 shows a proposed interaction between the hydrazide group on the POHQ polymers and hydroxyl groups formed by plasma treating the PDMS. This was obtained using ChemDraw 3D and using the dynamics function to observe interactions between the molecules by increasing the heat by 1 degree per second. This caused the hydrogen in the hydroxyl group to be attracted to the oxygen of the acyl group from the hydrazide. After this was observed, the minimize function was used to find the most likely arrangement of these molecules. Figure 21 shows the minimized reaction, in which the hydrogen of the hydroxyl group is electrostatically attracted to the acyl group of the hydrazide. This reaction hypothesis is likely why the microgel-PDMS is not

very strong, indicated through vortexing. Individual hydrogen bonds are not very strong and can be broken easily by mechanical forces such as vortexing (Halder et al., 2019).

4.2 Microgel-coated PDMS Antibacterial Properties

The coated condition showed effective sanitization of the PDMS surface (Altapure, 2024), indicating that this coating could be used as an antibacterial coating for PDMS. The vortexed condition showed a 42% increase in growth which was unexpected. This shows that the microgel-PDMS bonds are not highly stable. The increase in bacterial growth is likely due to increased bacterial binding to the surface. *S. aureus*. This species has been observed to bind to hydrophobic surfaces with many low-affinity macromolecules but bind to hydrophilic surfaces with a small number of high-affinity macromolecules (Maikranz et al., 2020). The vortex treatment on the coated PDMS likely left functional groups from plasma treatment (hydroxyl groups) and possibly microgel-binding (polar acyl groups). Since PDMS is naturally hydrophobic, these effects would cause the presence of both hydrophobic and hydrophilic areas. Thus, *S. aureus* could be using a multitude of ligand types to combine their natural adhesion to hydrophobic and hydrophilic surfaces. *S. aureus* was the only bacteria used for this test due to time constraints and because the microgels were slightly more effective against Gram-positive bacteria. Through testing with *P. aeruginosa*, it is possible that this observation would likely be less exacerbated. This is hypothesized because *P. aeruginosa* binds to hydrophobic surfaces with high affinity, but to hydrophilic surfaces with lower affinity (Zabielska et al., 2017). Thus, the creation of hydrophilic functional groups on the PDMS surface would likely decrease its binding and make it more difficult for these bacteria to adhere. Despite these unexpected results, the microgels can sanitize the surface of PDMS showing a 95% reduction in *S. aureus* growth from the coated condition.

This could be applied to food processing equipment surfaces containing PDMS to reduce biofilm formation.

Since the antibacterial test from microgel-binding was unexpected for the vortexed condition, a visual BPB stability test was used. Figure 20 shows no major differences in the residual BPB left over in the vortexed condition compared to the non-vortexed condition. Quantification of the number of microgels bound to the surface of these samples were not obtained. Thus, this test is inconclusive in that sense. However, since there are only slight visual differences between the vortexed and non-vortexed conditions, the microgel-PDMS bond may actually be more stable than indicated in the antibacterial tests. Further research is needed to assess the stability of the bond and how many microgels have been added to the surface.

4.3 Future Directions

While this study has shown a promising proof of concept, there are areas that should be explored further. The first of which is the stability of the microgels. While the microgels have been observed to be stable at just under 3 weeks, their stability should be assessed for longer periods of time. The storage of cleaners and disinfectants can last for years before they are used, thus, it is important to assess if the microgels can still perform their function over time. This includes antibacterial testing of the microgels over time. This was not completed in this study due to time constraints but could yield information of the activity of the microgels over time.

The next limitation is the inherent cytotoxicity of QAC-functionalized microgels. This is problematic in regard to medical applications and should be rectified if they are to be used in this fashion. It is possible that the use of other biocidal compounds could be used to reduce cytotoxicity. For example, perhaps the use of other biocidal agents such as tertiary sulfonium, phosphonium,

and guanidium could be used (Naeem et al., 2023). These are widely used biocidal agents added as functional groups on polymers and could exhibit less cytotoxicity (Naeem et al., 2023). Thus, testing POEGMA polymers with different biocidal functional groups could reduce cytotoxicity while maintaining antimicrobial properties. It may also be beneficial to observe the reduction of bacteria using microgels as a surface cleaner for PDMS, or other surfaces. Antibacterial properties of the microgels on their own was only assessed using serial dilutions in media. Therefore, investigating the contact killing of the microgels on various surfaces such as metals, plastics and other hard polymer structures, as well as other biomaterials such as extracellular matrix proteins could help establish these microgels as a surface cleaner (Hanawa, 2012; Wang, 2023).

Further research should be done to understand the bonding mechanism and stability between the microgels and the PDMS. This study only presented qualitative results, showing a proof of concept. However, methods to quantify the amount of microgel bound to the surface could be explored. For example, the use of spectrophotometry in combination with bromophenol blue could be used to measure the density of microgels deposited on the surface of PDMS. By measuring the absorbance of blue light (same as the dye), any deposited microgels will scatter the incoming light, meaning less absorbance could be observed. Additionally, coating the PDMS evenly with the microgels could be completed through spin or blade coating (Buratti et al., 2020). This would ensure that the whole surface of the PDMS is covered, maximizing the antibacterial surface area. Another way to evenly coat the microgels could be completed through electrospinning, however, the previous methods are simpler (Piperno et al., 2009). This could also help reduce the variation in patterns seen in the AFM images. The drying for evenly spread microgels would most likely occur at the same rate, causing uniform deposition of the microgels across the surface.

Antibacterial tests of microgel-coated PDMS should be completed with *P. aeruginosa* and possibly with other biofilm forming microbes. For example, *E. coli*, *Enterococcus faecalis*, *S. epidermis*, *Candida spp.*, *Aspergillus spp.*, and *Pneumocystis spp.* are microbes that form biofilms (Kernien et al., 2018; Khatoon et al., 2018). These could reveal the effectiveness of these microgels (with some variations in biocidal groups) against other biofilm-forming organisms.

Finally, the stability of the microgel-PDMS bond should be assessed using various techniques to mimic medical implant stress. For example, stability should be assessed using shearing, stretching, compression, and extended time in slightly acidic environments (to mimic urine for catheters). Once this is completed, more antibacterial tests of the PDMS surface coating should be completed, specifically over time. This will also give another measure of the stability between the microgels and PDMS. Of course, the toxicity would need to be addressed before this testing, but it is important, nonetheless. Overall, the preliminary results of this study prove that QAC-functionalized microgels can bond to PDMS and still exhibit antimicrobial properties. Further research should focus on the more technical aspects such as microgel stability, reducing cytotoxicity while maintaining antimicrobial properties, and microgel-PDMS bond stability.

5. Conclusion

Biofilms are an important consideration in medical applications and food processing industries due to their ability to resist antibiotic treatments. While there are many biofilm-forming microbes, this study focused on two major species: *S. aureus* and *P. aeruginosa*. A notable surface used in these applications that is notoriously known to host biofilms is PDMS. To prevent bacterial adhesion and reduce bacterial growth on PDMS, QAC-functionalized POEGMA microgels were synthesized and coated on PDMS. This proof-of-concept study showed that these microgels in

suspension are stable overtime in MiQ and PBS over a three-week period, indicating they could be stored for extended periods of time. The microgels in suspension were effective in disinfecting *S. aureus* and *P. aeruginosa* indicated by log reductions of 9.56 and 8.5, respectively. Furthermore, the microgels were able to bind to the surface of plasma-treated PDMS, indicated by residual BPB and surface morphology differences observed through AFM. The microgel-coated PDMS showed 95% reduction in *S. aureus*, indicating that it is still an effective antimicrobial. Finally, visual BPB stability tests for the strength of the microgel-PDMS bond was inconclusive but shows promise. This microgel coating is a feasible approach to reducing biofilm formation in applications such as food processing and microfluidics. Further research should be done to increase microgel-PDMS binding, as well as minimizing cytotoxicity if these are to be used in medical applications. Overall, these microgels could help reduce infections and combat antibiotic resistance by reducing biofilm formation on surfaces with PDMS, or even as a surface disinfectant.

References

Abebe, G. M. (2020). The Role of Bacterial Biofilm in Antibiotic Resistance and Food Contamination. *International Journal of Microbiology*, *2020*, 1705814. https://doi.org/10.1155/2020/1705814

Alberts, B., Johnson, A., Lewis, J., Raff, M., Roberts, K., & Walter, P. (2002). Looking at the Structure of Cells in the Microscope. In *Molecular Biology of the Cell. 4th edition*. Garland Science. https://www.ncbi.nlm.nih.gov/books/NBK26880/

Alihosseini, F., & Sun, G. (2011). 17—Antibacterial colorants for textiles. In N. Pan & G. Sun (Eds.), *Functional Textiles for Improved Performance, Protection and Health* (pp. 376–403). Woodhead Publishing. https://doi.org/10.1533/9780857092878.376

Altapure. (2024). *Altapure*. Altapure. https://altapure.com/log-reduction/

Alves, P. M., Al-Badi, E., Withycombe, C., Jones, P. M., Purdy, K. J., & Maddocks, S. E. (2018). Interaction between Staphylococcus aureus and Pseudomonas aeruginosa is beneficial for colonisation and pathogenicity in a mixed biofilm. *Pathogens and Disease*, *76*(1), fty003. https://doi.org/10.1093/femspd/fty003

Ansari, M. J., Rajendran, R. R., Mohanto, S., Agarwal, U., Panda, K., Dhotre, K., Manne, R., Deepak, A., Zafar, A., Yasir, M., & Pramanik, S. (2022). Poly(N-isopropylacrylamide)-Based Hydrogels for Biomedical Applications: A Review of the State-of-the-Art. *Gels*, *8*(7), 454. https://doi.org/10.3390/gels8070454

Armugam, A., Teong, S. P., Lim, D. S. W., Chan, S. P., Yi, G., Yew, D. S., Beh, C. W., & Zhang, Y. (2021). Broad spectrum antimicrobial PDMS-based biomaterial for catheter fabrication. *Biomaterials Research*, *25*, 33. https://doi.org/10.1186/s40824-021-00235-5

Arnold, W. A., Blum, A., Branyan, J., Bruton, T. A., Carignan, C. C., Cortopassi, G., Datta, S., DeWitt, J., Doherty, A.-C., Halden, R. U., Harari, H., Hartmann, E. M., Hrubec, T. C., Iyer, S., Kwiatkowski, C. F., LaPier, J., Li, D., Li, L., Muñiz Ortiz, J. G., … Zheng, G. (2023). Quaternary Ammonium Compounds: A Chemical Class of Emerging Concern. *Environmental Science & Technology*, *57*(20), 7645–7665. https://doi.org/10.1021/acs.est.2c08244

Assefa, M., & Amare, A. (2022). Biofilm-Associated Multi-Drug Resistance in Hospital-Acquired Infections: A Review. *Infection and Drug Resistance*, *15*, 5061–5068. https://doi.org/10.2147/IDR.S379502

Buratti, E., Sanzari, I., Dinelli, F., Prodromakis, T., & Bertoldo, M. (2020). Formation and Stability of Smooth Thin Films with Soft Microgels Made of Poly(N-Isopropylacrylamide) and Poly(Acrylic Acid). *Polymers*, *12*(11), 2638. https://doi.org/10.3390/polym12112638

Camagay, A. V., Kendall, N., & Connolly, M. K. (2024). Quaternary Ammonium Compound Toxicity. In *StatPearls*. StatPearls Publishing. http://www.ncbi.nlm.nih.gov/books/NBK594254/

Carrascosa, C., Raheem, D., Ramos, F., Saraiva, A., & Raposo, A. (2021). Microbial Biofilms in the Food Industry—A Comprehensive Review. *International Journal of Environmental Research and Public Health*, *18*(4), Article 4. https://doi.org/10.3390/ijerph18042014

Cont, A., Vermeil, J., & Persat, A. (2023). Material Substrate Physical Properties Control Pseudomonas aeruginosa Biofilm Architecture. *mBio*, *14*(2), e03518-22. https://doi.org/10.1128/mbio.03518-22

Costa, D. de M., Lopes, L. K. de O., Hu, H., Tipple, A. F. V., & Vickery, K. (2017). Alcohol fixation of bacteria to surgical instruments increases cleaning difficulty and may

contribute to sterilization inefficacy. *American Journal of Infection Control*, *45*(8), e81–e86. https://doi.org/10.1016/j.ajic.2017.04.286

de Lima, C. S. A., Balogh, T. S., Varca, J. P. R. O., Varca, G. H. C., Lugão, A. B., A. Camacho-Cruz, L., Bucio, E., & Kadlubowski, S. S. (2020). An Updated Review of Macro, Micro, and Nanostructured Hydrogels for Biomedical and Pharmaceutical Applications. *Pharmaceutics*, *12*(10), 970. https://doi.org/10.3390/pharmaceutics12100970

De Luca, M., Gaglione, R., Della Ventura, B., Cesaro, A., Di Girolamo, R., Velotta, R., & Arciello, A. (2022). Loading of Polydimethylsiloxane with a Human ApoB-Derived Antimicrobial Peptide to Prevent Bacterial Infections. *International Journal of Molecular Sciences*, *23*(9), 5219. https://doi.org/10.3390/ijms23095219

Di Martino, P. (2018). Extracellular polymeric substances, a key element in understanding biofilm phenotype. *AIMS Microbiology*, *4*(2), 274–288. https://doi.org/10.3934/microbiol.2018.2.274

Dieuzy, E., Auguste, S., Chougrani, K., Alard, V., Billon, L., & Derail, C. (2021). Microgel structure-driven linear and non-linear mechanical properties of self-assembled microgel films. *Colloids and Surfaces A: Physicochemical and Engineering Aspects*, *613*, 126082. https://doi.org/10.1016/j.colsurfa.2020.126082

Ding, H. X., Leverett, C. A., Kyne, R. E., Liu, K. K.-C., Fink, S. J., Flick, A. C., & O'Donnell, C. J. (2015). Synthetic approaches to the 2013 new drugs. *Bioorganic & Medicinal Chemistry*, *23*(9), 1895–1922. https://doi.org/10.1016/j.bmc.2015.02.056

Donlan, R. M. (2002). Biofilms: Microbial Life on Surfaces. *Emerging Infectious Diseases*, *8*(9), 881–890. https://doi.org/10.3201/eid0809.020063

Elias, S., & Banin, E. (2012). Multi-species biofilms: Living with friendly neighbors. *FEMS Microbiology Reviews*, *36*(5), 990–1004. https://doi.org/10.1111/j.1574-6976.2012.00325.x

Else, T. A., Pantle, C. R., & Amy, P. S. (2003). Boundaries for Biofilm Formation: Humidity and Temperature. *Applied and Environmental Microbiology*, *69*(8), 5006–5010. https://doi.org/10.1128/AEM.69.8.5006-5010.2003

Fux, C. A., Costerton, J. W., Stewart, P. S., & Stoodley, P. (2005). Survival strategies of infectious biofilms. *Trends in Microbiology*, *13*(1), 34–40. https://doi.org/10.1016/j.tim.2004.11.010

Gordon, V. D., & Wang, L. (2019). Bacterial mechanosensing: The force will be with you, always. *Journal of Cell Science*, *132*(7), jcs227694. https://doi.org/10.1242/jcs.227694

Guan, Y., & Zhang, Y. (2011). PNIPAM microgels for biomedical applications: From dispersed particles to 3D assemblies. *Soft Matter*, *7*(14), 6375–6384. https://doi.org/10.1039/C0SM01541E

Halder, A., Data, D., Seelam, P. P., Bhattacharyya, D., & Mitra, A. (2019). Estimating Strengths of Individual Hydrogen Bonds in RNA Base Pairs: Toward a Consensus between Different Computational Approaches. *ACS Omega*, *4*(4), 7354–7368. https://doi.org/10.1021/acsomega.8b03689

Hamadi, F., Latrache, H., Zahir, H., Elghmari, A., Timinouni, M., & Ellouali, M. (2008). The relation between Escherichia coli surface functional groups' composition and their physicochemical properties. *Brazilian Journal of Microbiology*, *39*(1), 10–15. https://doi.org/10.1590/S1517-83822008000100003

Hanawa, T. (2012). Research and development of metals for medical devices based on clinical needs. *Science and Technology of Advanced Materials*, *13*(6), 064102. https://doi.org/10.1088/1468-6996/13/6/064102

Hu, X., Tong, Z., & Lyon, L. A. (2011). Control of Poly(N-isopropylacrylamide) Microgel Network Structure by Precipitation Polymerization near the Lower Critical Solution Temperature. *Langmuir : The ACS Journal of Surfaces and Colloids*, *27*(7), 4142–4148. https://doi.org/10.1021/la200114s

Jain, K., Vedarajan, R., Watanabe, M., Ishikiriyama, M., & Matsumi, N. (2015). Tunable LCST behavior of poly(N-isopropylacrylamide/ionic liquid) copolymers. *Polymer Chemistry*, *6*(38), 6819–6825. https://doi.org/10.1039/C5PY00998G

Jefferson, K. K. (2004). What drives bacteria to produce a biofilm? *FEMS Microbiology Letters*, *236*(2), 163–173. https://doi.org/10.1111/j.1574-6968.2004.tb09643.x

Jesmer, A. H., Marple, A. S. T., & Wylie, R. G. (2023). Controlled swelling of biomaterial devices for improved antifouling polymer coatings. *Scientific Reports*, *13*(1), 19950. https://doi.org/10.1038/s41598-023-47192-8

Jia, Z., shen, D., & Xu, W. (2001). Synthesis and antibacterial activities of quaternary ammonium salt of chitosan. *Carbohydrate Research*, *333*(1), 1–6. https://doi.org/10.1016/S0008-6215(01)00112-4

Kernien, J. F., Snarr, B. D., Sheppard, D. C., & Nett, J. E. (2018). The Interface between Fungal Biofilms and Innate Immunity. *Frontiers in Immunology*, *8*. https://doi.org/10.3389/fimmu.2017.01968

Keskin, D., Tromp, L., Mergel, O., Zu, G., Warszawik, E., van der Mei, H. C., & van Rijn, P. (2020). Highly Efficient Antimicrobial and Antifouling Surface Coatings with Triclosan-

Loaded Nanogels. *ACS Applied Materials & Interfaces*, *12*(52), 57721–57731. https://doi.org/10.1021/acsami.0c18172

Khatoon, Z., McTiernan, C. D., Suuronen, E. J., Mah, T.-F., & Alarcon, E. I. (2018). Bacterial biofilm formation on implantable devices and approaches to its treatment and prevention. *Heliyon*, *4*(12), e01067. https://doi.org/10.1016/j.heliyon.2018.e01067

Knobloch, J. K.-M., Tofern, S., Kunz, W., Schütze, S., Riecke, M., Solbach, W., & Wuske, T. (2017). "Life-like" assessment of antimicrobial surfaces by a new touch transfer assay displays strong superiority of a copper alloy compared to silver containing surfaces. *PLoS ONE*, *12*(11), e0187442. https://doi.org/10.1371/journal.pone.0187442

Koçak, G., Tuncer, C., & Bütün, V. (2020). Stimuli-Responsive Polymers Providing New Opportunities for Various Applications. *Hacettepe Journal of Biology and Chemistry*, *48*(5), Article 5. https://doi.org/10.15671/hjbc.811267

Kumar, R., & Kumar Sahani, A. (2021). Role of superhydrophobic coatings in biomedical applications. *Materials Today: Proceedings*, *45*, 5655–5659. https://doi.org/10.1016/j.matpr.2021.02.457

Kvich, L., Burmølle, M., Bjarnsholt, T., & Lichtenberg, M. (2020). Do Mixed-Species Biofilms Dominate in Chronic Infections?–Need for in situ Visualization of Bacterial Organization. *Frontiers in Cellular and Infection Microbiology*, *10*, 396. https://doi.org/10.3389/fcimb.2020.00396

Lee, S., A. M., T., Cho, G., & Lee, J. (2022). Control of the Drying Patterns for Complex Colloidal Solutions and Their Applications. *Nanomaterials*, *12*(15), Article 15. https://doi.org/10.3390/nano12152600

Lewis, K. (2008). Multidrug Tolerance of Biofilms and Persister Cells. In T. Romeo (Ed.), *Bacterial Biofilms* (pp. 107–131). Springer. https://doi.org/10.1007/978-3-540-75418-3_6

Li, G., Varga, I., Kardos, A., Dobryden, I., & Claesson, P. M. (2021). Temperature-Dependent Nanomechanical Properties of Adsorbed Poly-NIPAm Microgel Particles Immersed in Water. *Langmuir*, *37*(5), 1902–1912. https://doi.org/10.1021/acs.langmuir.0c03386

Liu, L., & Sheardown, H. (2005). Glucose permeable poly (dimethyl siloxane) poly (*N*-isopropyl acrylamide) interpenetrating networks as ophthalmic biomaterials. *Biomaterials*, *26*(3), 233–244. https://doi.org/10.1016/j.biomaterials.2004.02.025

Liu, X., Yao, H., Zhao, X., & Ge, C. (2023). Biofilm Formation and Control of Foodborne Pathogenic Bacteria. *Molecules*, *28*(6), 2432. https://doi.org/10.3390/molecules28062432

Maikranz, E., Spengler, C., Thewes, N., Thewes, A., Nolle, F., Jung, P., Bischoff, M., Santen, L., & Jacobs, K. (2020). Different binding mechanisms of Staphylococcus aureus to hydrophobic and hydrophilic surfaces. *Nanoscale*, *12*(37), 19267–19275. https://doi.org/10.1039/D0NR03134H

Miranda, I., Souza, A., Sousa, P., Ribeiro, J., Castanheira, E. M. S., Lima, R., & Minas, G. (2021). Properties and Applications of PDMS for Biomedical Engineering: A Review. *Journal of Functional Biomaterials*, *13*(1), 2. https://doi.org/10.3390/jfb13010002

Mishra, R., Panda, A. K., De Mandal, S., Shakeel, M., Bisht, S. S., & Khan, J. (2020). Natural Anti-biofilm Agents: Strategies to Control Biofilm-Forming Pathogens. *Frontiers in Microbiology*, *11*. https://doi.org/10.3389/fmicb.2020.566325

Mohapatra, S., Yutao, L., Goh, S. G., Ng, C., Luhua, Y., Tran, N. H., & Gin, K. Y.-H. (2023). Quaternary ammonium compounds of emerging concern: Classification, occurrence, fate,

toxicity and antimicrobial resistance. *Journal of Hazardous Materials*, *445*, 130393. https://doi.org/10.1016/j.jhazmat.2022.130393

Muhammad, M. H., Idris, A. L., & Huang, T. (2020). Beyond Risk: Bacterial Biofilms and Their Regulating Approaches. *Frontiers in Microbiology*, *11*. https://doi.org/10.3389/fmicb.2020.00928

Naeem, N., Zafar, N., & Wahid, F. (2023). Chapter 7—Antimicrobial Green Composites. In Dr. Inamuddin & T. Altalhi (Eds.), *Green Sustainable Process for Chemical and Environmental Engineering and Science* (pp. 187–206). Elsevier. https://doi.org/10.1016/B978-0-323-95169-2.00012-2

Nastyshyn, S., Raczkowska, J., Stetsyshyn, Y., Orzechowska, B., Bernasik, A., Shymborska, Y., Brzychczy-Włoch, M., Gosiewski, T., Lishchynskyi, O., Ohar, H., Ochońska, D., Awsiuk, K., & Budkowski, A. (2020). Non-cytotoxic, temperature-responsive and antibacterial POEGMA based nanocomposite coatings with silver nanoparticles. *RSC Advances*, *10*(17), 10155–10166. https://doi.org/10.1039/c9ra10874b

Niculescu, A.-G., Chircov, C., Bîrcă, A. C., & Grumezescu, A. M. (2021). Fabrication and Applications of Microfluidic Devices: A Review. *International Journal of Molecular Sciences*, *22*(4), 2011. https://doi.org/10.3390/ijms22042011

Pan, F., Zhang, S., Altenried, S., Zuber, F., Chen, Q., & Ren, Q. (2022). Advanced antifouling and antibacterial hydrogels enabled by controlled thermo-responses of a biocompatible polymer composite. *Biomaterials Science*, *10*(21), 6146–6159. https://doi.org/10.1039/D2BM01244H

Peppas, N. A., Hilt, J. Z., Khademhosseini, A., & Langer, R. (2006). Hydrogels in Biology and Medicine: From Molecular Principles to Bionanotechnology. *Advanced Materials*, *18*(11), 1345–1360. https://doi.org/10.1002/adma.200501612

Piperno, S., Gheber, L. A., Canton, P., Pich, A., Dvorakova, G., & Biffis, A. (2009). Microgel electrospinning: A novel tool for the fabrication of nanocomposite fibers. *Polymer*, *50*(26), 6193–6197. https://doi.org/10.1016/j.polymer.2009.11.004

Ribeiro, M. M., Neumann, V. A., Padoveze, M. C., & Graziano, K. U. (2015). Efficacy and effectiveness of alcohol in the disinfection of semi-critical materials: A systematic review. *Revista Latino-Americana de Enfermagem*, *23*(4), 741–752. https://doi.org/10.1590/0104-1169.0266.2611

Romeu, M. J., & Mergulhão, F. (2023). Development of Antifouling Strategies for Marine Applications. *Microorganisms*, *11*(6), 1568. https://doi.org/10.3390/microorganisms11061568

Schrank, C. L., Minbiole, K. P. C., & Wuest, W. M. (2020). Are Quaternary Ammonium Compounds, the Workhorse Disinfectants, Effective against Severe Acute Respiratory Syndrome-Coronavirus-2? *ACS Infectious Diseases*, *6*(7), 1553–1557. https://doi.org/10.1021/acsinfecdis.0c00265

Simpson, M. J., Corbett, B., Arezina, A., & Hoare, T. (2018). Narrowly Dispersed, Degradable, and Scalable Poly(oligoethylene glycol methacrylate)-Based Nanogels via Thermal Self-Assembly. *Industrial & Engineering Chemistry Research*, *57*(22), 7495–7506. https://doi.org/10.1021/acs.iecr.8b00793

Smeets, N. M. B., Bakaic, E., Patenaude, M., & Hoare, T. (2014). Injectable poly(oligoethylene glycol methacrylate)-based hydrogels with tunable phase transition

behaviours: Physicochemical and biological responses. *Acta Biomaterialia*, *10*(10), 4143–4155. https://doi.org/10.1016/j.actbio.2014.05.035

Stepulane, A., Rajasekharan, A. K., & Andersson, M. (2022). Multifunctional Surface Modification of PDMS for Antibacterial Contact Killing and Drug-Delivery of Polar, Nonpolar, and Amphiphilic Drugs. *ACS Applied Bio Materials*, *5*(11), 5289. https://doi.org/10.1021/acsabm.2c00705

Stoodley, P., Sauer, K., Davies, D. G., & Costerton, J. W. (2002). Biofilms as Complex Differentiated Communities. *Annual Review of Microbiology*, *56*(Volume 56, 2002), 187–209. https://doi.org/10.1146/annurev.micro.56.012302.160705

Subhadra, B., Kim, D. H., Woo, K., Surendran, S., & Choi, C. H. (2018). Control of Biofilm Formation in Healthcare: Recent Advances Exploiting Quorum-Sensing Interference Strategies and Multidrug Efflux Pump Inhibitors. *Materials*, *11*(9), 1676. https://doi.org/10.3390/ma11091676

Sun, W., Liu, J., Hao, Q., Lu, K., Wu, Z., & Chen, H. (2022). A novel Y-shaped photoiniferter used for the construction of polydimethylsiloxane surfaces with antibacterial and antifouling properties. *Journal of Materials Chemistry B*, *10*(2), 262–270. https://doi.org/10.1039/D1TB01968F

Tu, Q., Zhang, Q., Wang, Y., Jiao, Y., Xiao, J., Peng, T., & Wang, J. (2019). Antibacterial properties of poly(dimethylsiloxane) surfaces modified with graphene oxide-catechol composite. *Progress in Organic Coatings*, *129*, 247–253. https://doi.org/10.1016/j.porgcoat.2019.01.011

Utari, P. D., Setroikromo, R., Melgert, B. N., & Quax, W. J. (2018). PvdQ Quorum Quenching Acylase Attenuates Pseudomonas aeruginosa Virulence in a Mouse Model of

Pulmonary Infection. *Frontiers in Cellular and Infection Microbiology*, *8*. https://doi.org/10.3389/fcimb.2018.00119

van Poll, M. L., Zhou, F., Ramstedt, M., Hu, L., & Huck, W. T. S. (2007). A Self-Assembly Approach to Chemical Micropatterning of Poly(dimethylsiloxane). *Angewandte Chemie International Edition*, *46*(35), 6634–6637. https://doi.org/10.1002/anie.200702286

Vihola, H., Laukkanen, A., Valtola, L., Tenhu, H., & Hirvonen, J. (2005). Cytotoxicity of thermosensitive polymers poly(*N*-isopropylacrylamide), poly(*N*-vinylcaprolactam) and amphiphilically modified poly(*N*-vinylcaprolactam). *Biomaterials*, *26*(16), 3055–3064. https://doi.org/10.1016/j.biomaterials.2004.09.008

Vogel, J., Wakker-Havinga, M., Setroikromo, R., & Quax, W. J. (2020). Immobilized Acylase PvdQ Reduces Pseudomonas aeruginosa Biofilm Formation on PDMS Silicone. *Frontiers in Chemistry*, *8*. https://doi.org/10.3389/fchem.2020.00054

Wang, H. (2023). Biomaterials in Medical Applications. *Polymers*, *15*(4), 847. https://doi.org/10.3390/polym15040847

Wechsler, M. E., Stephenson, R. E., Murphy, A. C., Oldenkamp, H. F., Singh, A., & Peppas, N. A. (2019). Engineered microscale hydrogels for drug delivery, cell therapy, and sequencing. *Biomedical Microdevices*, *21*(2), 31. https://doi.org/10.1007/s10544-019-0358-0

Wu, H., Moser, C., Wang, H.-Z., Høiby, N., & Song, Z.-J. (2015). Strategies for combating bacterial biofilm infections. *International Journal of Oral Science*, *7*(1), 1–7. https://doi.org/10.1038/ijos.2014.65

Xu, X., Liu, Y., Fu, W., Yao, M., Ding, Z., Xuan, J., Li, D., Wang, S., Xia, Y., & Cao, M. (2020). Poly(N-isopropylacrylamide)-Based Thermoresponsive Composite Hydrogels for Biomedical Applications. *Polymers*, *12*(3), Article 3. https://doi.org/10.3390/polym12030580

Yang, B., Sharp, J. S., & Smith, M. I. (2016). The interplay of crack hopping, delamination and interface failure in drying nanoparticle films. *Scientific Reports*, *6*(1), 32296. https://doi.org/10.1038/srep32296

Zabielska, J., Kunicka-Styczyńska, A., & Otlewska, A. (2017). Adhesive and hydrophobic properties of Pseudomonas aeruginosa and Pseudomonas cedrina associated with cosmetics. *Ecological Questions*, *28*, 41–46. https://doi.org/10.12775/EQ.2017.037

Zhang, Q.-Y., Yan, Z.-B., Meng, Y.-M., Hong, X.-Y., Shao, G., Ma, J.-J., Cheng, X.-R., Liu, J., Kang, J., & Fu, C.-Y. (2021). Antimicrobial peptides: Mechanism of action, activity and clinical potential. *Military Medical Research*, *8*, 48. https://doi.org/10.1186/s40779-021-00343-2

Zhao, Z., Ma, X., Chen, R., Xue, H., Lei, J., Du, H., Zhang, Z., & Chen, H. (2020). Universal Antibacterial Surfaces Fabricated from Quaternary Ammonium Salt-Based PNIPAM Microgels. *ACS Applied Materials & Interfaces*, *12*(17), 19268–19276. https://doi.org/10.1021/acsami.0c00791

Zhong, W., Shi, Z., Mahadevegowda, S. H., Liu, B., Zhang, K., Koh, C. H., Ruan, L., Chen, Y., Zeden, M. S., Pee, C. J. E., Marimuthu, K., De, P. P., Ng, O. T., Zhu, Y., Chi, Y. R., Hammond, P. T., Yang, L., Gan, Y.-H., Pethe, K., … Chan-Park, M. B. (2020). Designer broad-spectrum polyimidazolium antibiotics. *Proceedings of the National Academy of Sciences*, *117*(49), 31376–31385. https://doi.org/10.1073/pnas.2011024117

Zhu, Y., McHale, G., Dawson, J., Armstrong, S., Wells, G., Han, R., Liu, H., Vollmer, W., Stoodley, P., Jakubovics, N., & Chen, J. (2022). Slippery Liquid-Like Solid Surfaces with Promising Antibiofilm Performance under Both Static and Flow Conditions. *ACS Applied Materials & Interfaces*, *14*(5), 6307–6319. https://doi.org/10.1021/acsami.1c14533

Zuppardi, F., Malinconico, M., d'Agosto, F., D'ayala, G. G., & Cerruti, P. (2020). Well-Defined Thermo-Responsive Copolymers Based on Oligo(Ethylene Glycol) Methacrylate and Pentafluorostyrene for the Removal of Organic Dyes from Water. *Nanomaterials*, *10*(9), 1779. https://doi.org/10.3390/nano10091779

Supplementary Figures

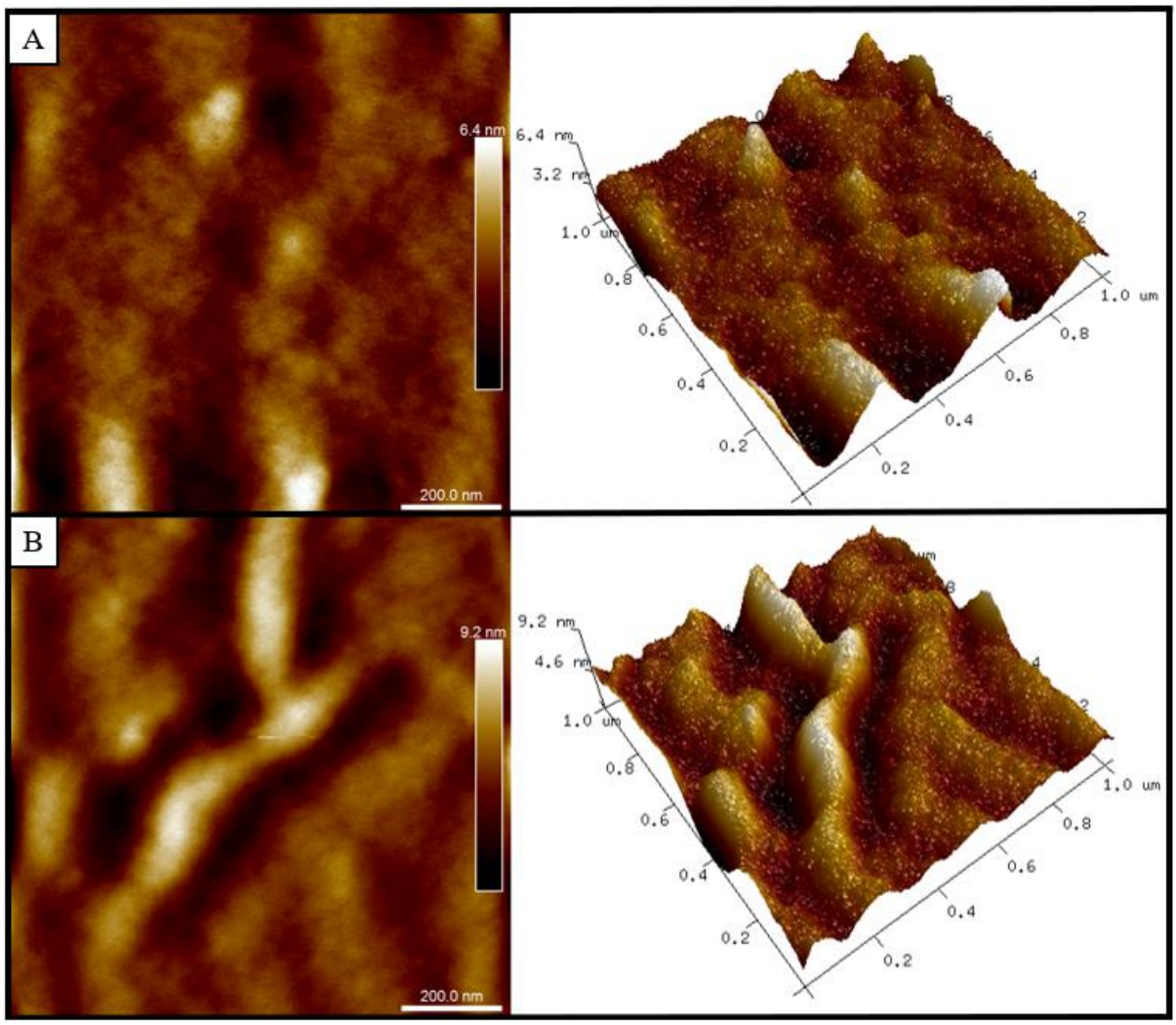

Supplementary Figure 1. AFM images of microgel coated PDMS. Panels A and B are both 1x1 μm images with a two-dimensional (left) and three-dimensional (right) representations. Higher morphologies are indicated by lighter colours, whereas lower morphologies have darker colours. These images show the wave-like patterns that formed after microgel drying on the PDMS surface.

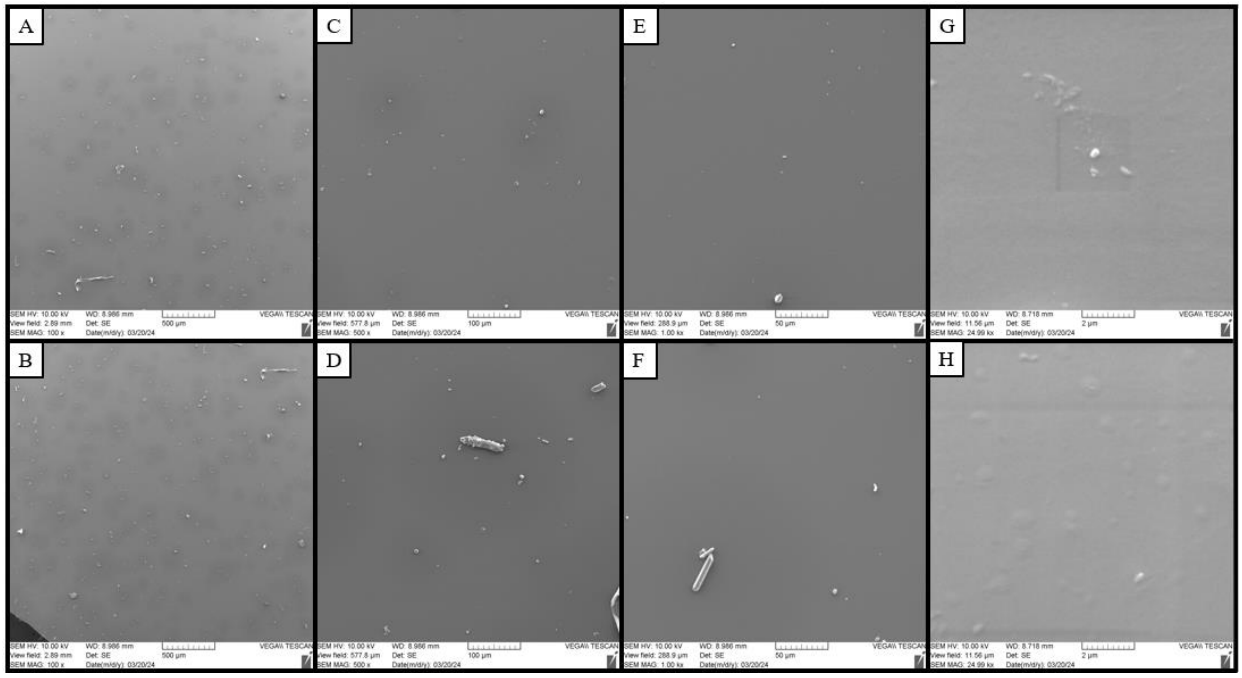

Supplementary Figure 2. SEM images of uncoated PDMS. Panels A and B, C and D, E and F, and G and H have magnifications of 100X, 500X, 1,000X, and 25,000X, respectively. All panels have visible particles on the PDMS. These are most likely dirt or dust.

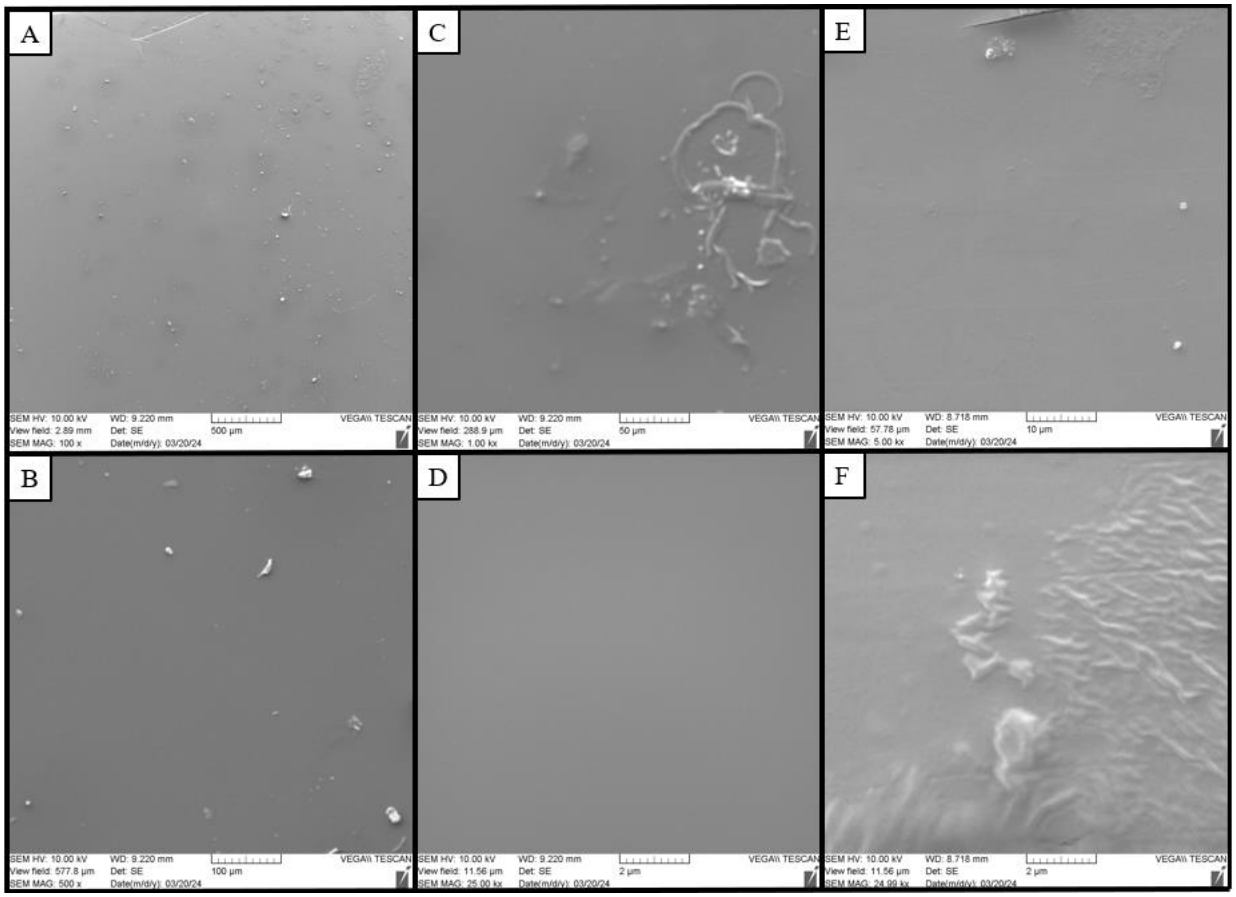

Supplementary Figure 3. SEM images of microgel coated PDMS. Panels A, B, C, and D are all from one coated sample which was accidentally dropped on the floor during preparation. Panels E and F are from another coated sample which was prepared as intended. The panels (in alphabetical order) have magnifications as follows: 100X, 500X, 1,000X, 25,000X, 5,000X, and 25,000X. There are film-like structures in panels E (top right) and F, which indicate something has coated the surface. However, this is inconclusive.

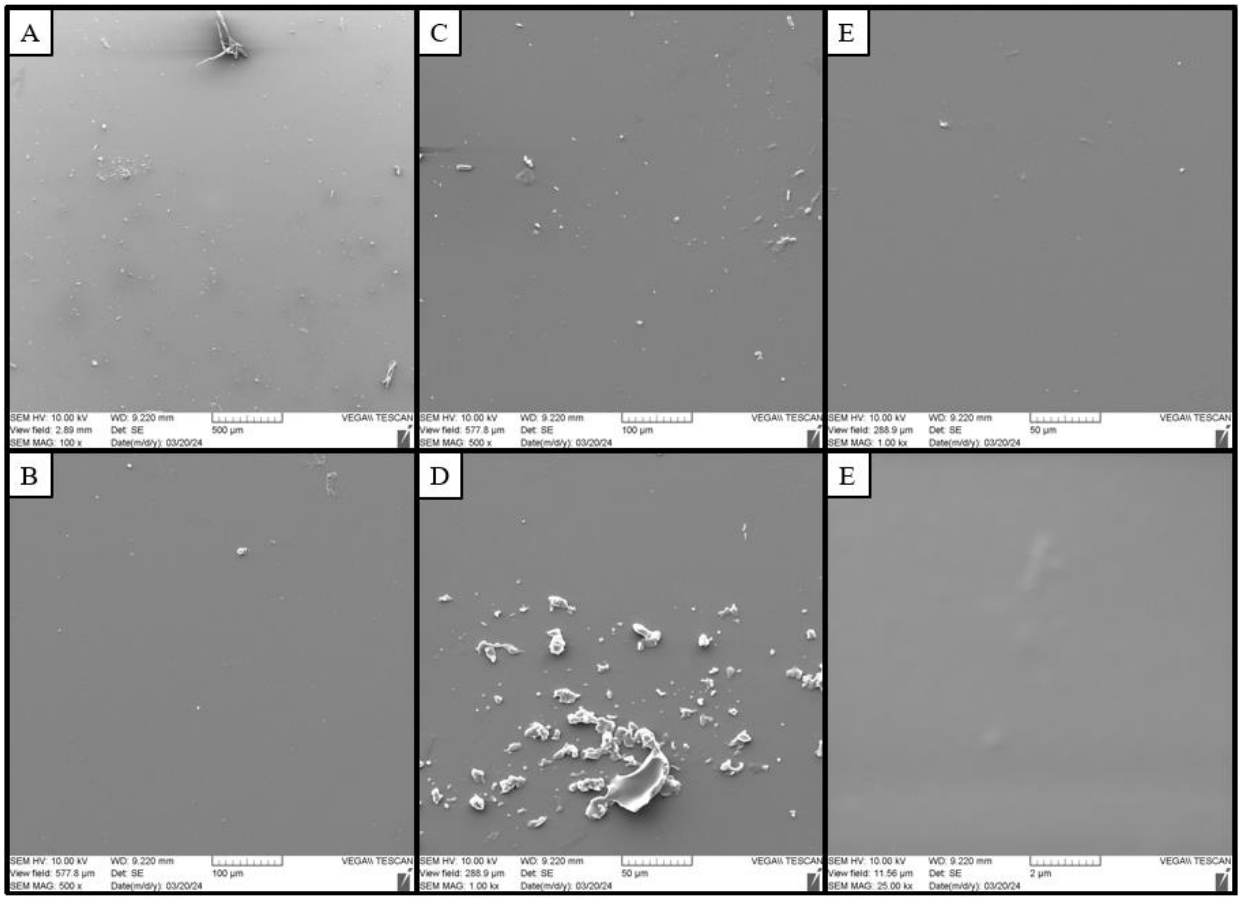

Supplementary Figure 4. SEM images of vortexed microgel coated PDMS. The panels (in alphabetical order) have magnifications as follows: 100X, 500X, 500X, 1,000X, 1,000X, and 25,000X. There are some particles scattered on the surface of this sample, however, they are likely not microgel aggregations. The resolution of the SEM was not precise enough to observe the microgels, thus, this is inconclusive for microgel binding.